

# **Optimization of Grounding Grids Design with Evolutionary Strategies**

Von der Fakultät Ingenieurwissenschaften der

Univeristät Duisburg-Essen

zur Erlangung des akademischen Grades eines

Doktor-Ingenieurs

genehmigte Dissertation

Von

**Sherif Salama Mohamed Ghoneim**

aus

**Kalubia-Ägypten**

Referent: Prof. Dr. Ing. Holger Hirsch

Korreferent: Prof. Dr. Ing. Ignasi Colominas

Tag der mündlichen Prüfung: 19.11.2007

# Abstract

In order to achieve lightning protection and electromagnetic compatibility (EMC) requirements, a proper grounding system is needed. Furthermore, the Earth Surface Potential (ESP) due to discharging current into grounding system in case of abnormal conditions has to be known.

The Main objectives of the grounding system are,

- I) To guarantee the integrity of the equipments and continuity of the service under the fault conditions (providing means to carry and dissipate electrical currents into ground).
- II) To safeguard those people that working or walking in the surroundings of the grounded installations are not exposed to dangerous electrical shocks.

To attain these targets, the equivalent electrical grounding resistance ( $R_g$ ) of the system must be low enough to assure that fault currents dissipate mainly through the grounding grid into the earth, while maximum potential difference between close points into the earth's surface must be kept under certain tolerances (step, touch, and mesh voltages).

A lot of efforts had been taken to answer the very important question, which is, how the Earth Surface Potential due to discharging current into grounding system can be calculated. Many researches are published to present information about step and touch voltages, some of these publications depend on the experimental works on a scale model and the other depend on some empirical function that depend also on the results from experimental.

Scale model in an electrolytic tank to simulate the lightning events on earth is presented to measure the Earth Surface Potential (ESP) on the surface of the water and also to study the transient performance of the grounding grid when it subjects to lightning like (Impulse current), in order to know something about the behaviour of the grid structure, i.e. is there a transient behaviour that needs complex models or is a static model sufficient and also give evidence to computer model. Impulse current tests were performed on 16(4 x 4) meshes.

On the other hand, an old, but still easy to implement technique depend on Charge Simulation Method (CSM) is proposed to calculate the fields with the equivalent charges, the attractiveness of the CSM, when compared with the Finite Element and Finite Difference Method emanates from its simplicity in representing the equipotential surfaces of the electrodes, its application to unbounded arrangements whose boundaries extend to infinity, its

direct determination to the electric field and its calculation speed. The results of the method are compared to experimental measurement results, empirical formulas in an IEEE standard and also to the other technique like (Boundary Element Method) that is often used to calculate Earth Surface Potential.

In the field of grounding system design, the optimization means to find a grounding system which is able to safeguard those people that working or walking in the surroundings of the grounded installations and on the other hand has minimal cost. A new technique combining Evolutionary Algorithm with CSM field computation is proposed for optimization the design of grounding grids. The basic design quantities of the grounding grids are the ground resistance ( $R_g$ ), touch voltage ( $V_t$ ), step voltage ( $V_s$ ) and the cost of the grounding system design. These mentioned quantities depend on the grid parameters, which are its side lengths, radius of grid conductors and length of vertical rods.

## Published papers

- [i] S. Ghoneim, H. Hirsch, A. Elmorshedy, R. Amer, “Improved Design of Square Grounding Grids”, International Conference Power System Technology, POWERCON2006, Chongqing, China, October 2006, pp. 1 – 4.
- [ii] S. Ghoneim, H. Hirsch, A. Elmorshedy, R. Amer, “Surface Potential Calculation for Grounding Grids”, IEEE International Power and Energy Conference, PEcon2006, Putra Jaya, Malaysia, November 2006, pp. 501 – 505.
- [iii] S. Ghoneim, H. Hirsch, A. Elmorshedy, R. Amer, “Effect of Profile Location on Step and Touch Voltages of Grounding Grids”, The Eleventh International Middle East Power Systems Conference, MEPCON2006, Elmenia, Egypt, December. 2006.
- [iv] S. Ghoneim, H. Hirsch, A. Elmorshedy, R. Amer, “Quality Model for Optimum Design of Grounding Grid”, 1<sup>st</sup> International Power Engineering and Optimization Conference, PEOCO2007, Shah Alam, Malaysia, June. 2007.
- [v] S. Ghoneim, H. Hirsch, A. Elmorshedy, R. Amer, “Optimum Grounding Grid Design by Using an Evolutionary Algorithm,” IEEE General Meeting, Tampa, Florida, USA, June 2007.
- [vi] S. Ghoneim, H. Hirsch, A. Elmorshedy, R. Amer, "Charge Simulation Method for Finding Step and Touch Voltage", 15<sup>th</sup> ISH2007, Slovenia, August 2007.
- [vii] S. Ghoneim, H. Hirsch, A. Elmorshedy, R. Amer, "Measurement of Earth Surface Potential Using Scale Model", UPEC2007, Brighton University, England, September 2007.

To my wife, my daughter, my son, my parents and all who have  
helped me

# Acknowledgements

On the occasion of finishing my PhD study, it gives me immense pleasure to express my gratitude to all the people who have supported me and contributed to my work.

I hope to submit my great thanks to Prof. Holger Hirsch, the head of the Energy Transmission and Storage Institute, Duisburg-Essen University, for all efforts, cooperations, supports and encouragements to finish this thesis. I did not find any words to express my feeling towards him but I think that he is a good father doctor for me.

I am grateful to one of my best guidance for the work, Prof. Ignasi Colominas from the Civil Engineering School of the University of La Coruna (Spain), for all his fruitful discussions, cooperations and encouragement during my study.

The help and assistance from all persons work in the Energy Transmission and Storage Institute- Duisburg-Essen University is greatly appreciated.

In the last, I would like to thank my wife for supporting me in all that I did. Also this thesis is written for my daughter and son, thanks for all persons in my wife's Family and a lot of thanks to my parents who pray for me to finish this thesis.

# Contents

<b>Chapter 1: Introduction</b>	<b>1</b>
1.1 The role of grounding systems in lightning protection	1
1.2 Overview of Earth Surface Potential calculation	5
1.2.1 Earth Surface Potential calculation using empirical formulas	5
1.2.2 Earth Surface Potential calculation using numerical methods	11
1.2.3 Earth Surface Potential calculation using scale model	13
<b>Chapter 2: Terminology and Definitions</b>	<b>17</b>
2.1 Definitions	17
<b>Chapter 3: Experimental Investigations</b>	<b>21</b>
3.1 Scale model with scaling time of the applied impulse current	21
3.2 Test setup	23
3.3 Test results	28
<b>Chapter 4: Methods of Calculation</b>	<b>36</b>
4.1 Boundary Element Method	36
4.2 Charge Simulation Method	38
<b>Chapter 5: Calculation Results</b>	<b>43</b>
5.1 Calculation results using BEM	43
5.1.1 Importance of vertical rods addition to grounding grid	43
5.1.2 Effect of the vertical rods location on the step and touch voltage	44
5.1.3 Effect of the profile location on the grid resistance, step and touch voltages	46
5.2 Calculation results using CSM	49
5.2.1 Effect of the number of meshes on the earth surface potential	49
5.2.2 Effect of the vertical rods and its length on the earth surface potential	50
5.2.3 Effect of grid depth on the earth surface potential	52
5.2.4 Effect of number of point charges on the earth surface potential	52
5.3 Validation of the Charge Simulation Method	53
5.4 Comparison between the experimental and theoretical calculation by (Charge Simulation Method)	55
<b>Chapter 6: Optimization of Grounding Grids Design Based on Evolutionary Strategy</b>	<b>58</b>

6.1	Evolutionary Algorithm (Optimizer)	59
6.2	Numerical Example	63
<b>Chapter 7: Conclusions</b>		66
<b>References</b>		69



## List of tables

Table (3-1) The average values of the measured voltage at specified points as in Fig. (3-8).	34
Table (5-1) Comparison between the additional of horizontal rods and vertical rods to the grounding grid.	44
Table (5-2) GPR, max step voltage, max touch voltage, grounding resistances for different cases.	46
Table (5-3) The values of ground grid resistance, step and touch voltages for the different profile locations of different configurations of grounding grids for fault current ( $I_f$ ) of 100 A.	48
Table (5-4) Comparison between the grounding resistance for Boundary Element Method and IEEE standard formulas.	49
Table (5-5) Comparison between the grounding resistance for the proposed method and the IEEE standard formulas and also the Boundary Element Method.	53
Table (5-6) Voltage differences at specified points as in Fig. (3-8).	56
Table (5-7) Comparison between the results from the proposed method and the scale model.	56
Table (6-1) Optimization design results.	63

# List of Figures

Fig. (1-1) Illustration of common grounding structure.	2
Fig. (1-2) Fibrillating current versus body weight for various animals based on a three second shock.	4
Fig. (1-3) Development of the potential around the rod.	6
Fig. (1-4) Field strength on the surface around a driven rod.	6
Fig. (1-5) Grounding grids under considerations.	7
Fig. (1-6) Earth Surface Potential profiles.	10
Fig. (1-7) Measurement circuit.	13
Fig. (1-8) The experimental setup.	14
Fig. (2-1) Illustration of the touch and step voltages for grounding grids.	19
Fig. (3-1) Schematic diagram for time scaling circuit.	22
Fig. (3-2) The waveform of the applied current with the proposed front to tail time $t_f/t_r=70/300$ ns.	23
Fig. (3-3) The impulse form at 12/500 ns.	23
Fig. (3-4a) The Electrolytic tank with water, grid and probs.	25
Fig. (3-4b) The Electrolytic tank with grid.	25
Fig. (3-5) Ultra compact Impulse generator.	26
Fig. (3-6) Oscilloscope type Tektronix -DPO4014.	26
Fig. (3-7) WTW Microprocessor Conductivity meter type LF2000.	27
Fig. (3-8) Configuration of grid that used as scale model.	27
Fig. (3-9) Scale time circuit.	28
Fig. (3-10) The probe used to measure the voltage difference between two points on the water surface.	29
Fig. (3-11) Reduction the length return current path.	29
Fig. (3-12) Elimination of the interference from external signal sources using metal housing.	30
Fig. (3-13a) Current (blue line) and the voltage difference between points 1 and 2 as in Fig. (3-8).	31
Fig. (3-13b) Current (blue line) and the voltage difference between points 1 and 2 as in Fig. (3-8) when changing the polarity of the voltage probe.	31
Fig. (3-14a) Current (blue line) and the voltage difference between points 2	

and 3 as in Fig. (3-8).	32
Fig. (3-14b) Current (blue line) and the voltage difference between points 2 and 3 as in Fig. (3-8) when changing the polarity of the voltage probe.	32
Fig. (3-15a) Current (blue line) and the voltage difference between points 3 and 4 as in Fig. (3-8).	33
Fig. (3-15b) Current (blue line) and the voltage difference between points 3 and 4 as in Fig. (3-8) when changing the polarity of the voltage probe.	33
Fig. (4-1) Illustration of CSM technique.	39
Fig. (5-1) Different grounding grids.	
(a) 36 meshes. (b) 4 meshes with vertical rods.	43
Fig. (5-2) Grounding grids with different meshes and different locations of the vertical rods (a. without vertical rods, b. with vertical rods at all point, c. the vertical rods at the points across the diagonal and center lines, d. the vertical rods at the perimeter of the grid only), the small circles indicate the location of the vertical rods.	45
Fig. (5-3) Grounding grids with different profile locations (a. square grids (20x20m) without vertical rods, b. square grids (20x20m) with vertical rods at all point, c. rectangle grids (10x40m) without vertical rods, d. rectangle grids (10x40m) with vertical rods at all point).	47
Fig. (5-4) Effect of number of meshes on earth surface potential.	50
Fig. (5-5) Effect of vertical rods addition to the grids on earth surface potential.	51
Fig. (5-6) Effect of vertical rods length to the grids on earth surface potential.	51
Fig. (5-7) Effect of grid depth on earth surface potential.	52
Fig. (5-8) Effect of number of point charges on earth surface potential.	53
Fig. (5-9) Comparison between proposed method and Boundary Element Method for 16 meshes grid without vertical rods.	54
Fig. (5-10) Comparison between proposed method and Boundary Element Method for 16 meshes grid with vertical rods (2m length).	54
Fig. (5-11) Earth Surface Potential profile for real model.	55

Fig. (6-1) Evolutionary Strategy model for optimization the design of grounding grids.	59
Fig. (6-2) Flow chart of the program based on evolutionary strategy to optimize the grounding grid design.	60
Fig. (6-3a, b, c) The relationships between the quality factors and (cost, $V_t$ , $V_s$ ).	62

## List of symbols

$R_g$  = grounding resistance

$V_t$  = touch voltage

$V_s$  = step voltage

$\rho$  = the soil resistivity in  $\Omega.m$

$t$  = the duration time that the current pass in the human body

$GPR$  = Ground Potential Rise

ESP = Earth Surface Potential

$V$  = the voltage at the earth surface

$I$  = the current flows into the rod

$l$  = the rod length and

$\beta$  = the angle between the axis of the rod and the distance from the rod to the point under consideration at the surface

$L$  = the total length of buried conductors

$K_m$  = the mesh factor defined for  $N$  parallel conductors,

$K_{mi}$  = the corrective factor for current irregularity

$h$  = depth in m

$d$  = the conductor diameter

$D$  = space between parallel conductors

$V_{mesh}$  = the mesh potential

$i_g$  = maximum rms current flowing between ground grid and earth

$V_{step}$  = the step potential

$K_s$  = the step factor defined for  $N$  parallel conductors,

$K_{si}$  = the corrective factor for current irregularity

$K_i$  = irregularity factor

$n$  = number of parallel rods in one direction

$C_I$  = constant

$a$  = the side length of the grid in m

$K_{mir}$  = the mesh factor of square grid with the same  $h$  and  $N$  and  $a$  equal to the grid side of the rectangle grid

$V_{my}$  = vertical component of mesh voltage

$V_{mx}$  = horizontal component of the mesh voltage

$V_{min}$  = the minimum surface potential in the grid boundary.

$L_{vr}$  = the length of vertical rods

$r_{vr}$  = vertical rod radius

$P_{ij}$  = the potential coefficients which can be evaluated analytically for many types of charges by solving Laplace or Poisson's equations

$\Phi_i$  = the potential at contour points

$Q_j$  = the charge at the point charges

$d_{ij}$  = the distance between the contour point i and charge point j

$C$  = the capacitance of the grounding grid (farad)

$Q_F$  = the total quality factor

$V_{tsl}, V_{ssl}$  = the safe limit of touch and step voltages at the case study

$X$  = the side length of the grid in x direction

$Y$  = the side length of the grid in y direction

$Z$  = the length of the vertical rod if available

$r$  = the grid conductor radius

$x_I$  = factor related to cost



# Chapter 1

## Introduction

### 1.1 The role of grounding systems in lightning protection

The earth has been used as a conductor for electric current since the beginning of engineering. However, after a brief period of performance for sending return currents through the ground, great difficulties and hazards were found from this in all branches of electrical engineering. One remaining application of earth for return currents is High Voltage DC transmission (HVDC).

Nowadays the earth is used mainly for fixing the neutral point of the electric system, and in many instances the inclusion of the earth as part of the circuit cannot be avoided. In the earth, the currents spread out in the entire space, and it is necessary to follow their paths in order to analyze their performance in the underground. These currents should be passing into easy paths, therefore, grounding systems are provided to decrease the resistance of the earth as low as possible.

One of tasks of the grounding systems is to maintain the voltage rise due to discharging fault current into grounding grids at the minimum value to insure the safety of public and personnel and to avoid as far as possible EMC problems due to galvanic coupling. Fig. (1-1) shows the commonly used grounding structures, namely, single horizontal grounding wire, vertical rode, ring conductor and grounding grid with large area.

Grounding grids are considered an effective solution for grounding systems for all sites which must be protected from lightning strokes such as, telecommunication towers, petroleum fields, substations and plants. Grounding grids produce an equipotential surfaces and should provide a very small impedance but the grounding grids are considered complex arrangement and many research efforts have been made to explain the performance of grounding impedance of its under lightning and fault conditions [1-16]. Vertical ground rods are the simplest and commonly used means for earth termination of electrical and lightning protection systems. The addition of the vertical ground rods to the grounding grid achieve a convenient design for grounding system to improve the performance of it by reducing not only the grid resistance but also the step and touch voltages to values that safe for human.



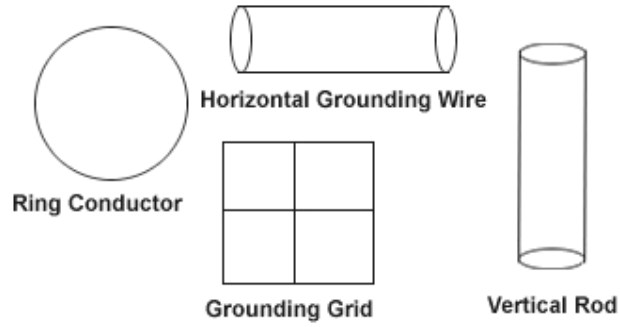


Fig. (1-1) Illustration of common grounding structure.

The objectives of adequate grounding system are summarized in the following points:

- 1- Creating an easy return path for the return stroke current that develops from lightning.
- 2- Reduction the breakdown risks on electrical and electronic equipments.
- 3- Achievement the minimum cost by continuity of the power systems.
- 4- Reduction the risks for human by decreasing the touch and step voltages which are the most important parameters for grounding system.

To attain these targets, the equivalent electrical resistance ( $R_g$ ) of the system must be low enough to assure that fault currents dissipate mainly through the grounding grid into the earth, while maximum potential difference between close points into the earth's surface must be kept under certain tolerances (step, touch, and mesh voltages) [17].

The important parameters from design grounding system are the touch and step voltages which should be at the safe value for human. The safety of a person depends on preventing the critical amount of shock energy from being absorbed before the fault is cleared and the system de-energized. The maximum driving voltage of any accident circuit should not exceed the limits defined below. The safe value for step voltage in Volt is given by the empirical formula:

$$V_{step} = (R_B + R_{2Fs})I_B \quad (1.1)$$

where,  $R_B$  is the human body resistance which assumes  $1000 \Omega$ ,  $R_{2Fs}$  is the resistance of the two feet in series and  $I_B$  is the rms magnitude of the current through the human body.

## Chapter 1: Introduction

$$R_{2Fs} = 2(R_{foot} - R_{Mfoot}) \quad (2.1)$$

$$\text{where, } R_{foot} = \frac{\rho_s}{4b} \text{ and } R_{Mfoot} = \frac{\rho_s}{2\pi d_F}$$

By neglecting the mutual resistance  $R_{Mfoot}$

$$R_{2Fs} = 6.0C_s(h_s, K)\rho_s$$

Where  $\rho_s$  is the soil resistivity in  $\Omega.m$ ,  $b$  is the radius of the conducting disc which simulates the foot and assumes 0.08 m,  $d_F$  is the distance between two feet and assumes 1 m,  $C_s$  is the factor depend on the thickness of the crushed rock surface ( $h_s$ ) and the reflection coefficient ( $K$ ) and  $C_s$  is equal to 1 for a homogenous soil. The permissible current can be calculated by the following equation;

$$I_B = \begin{cases} \frac{0.116}{\sqrt{t_s}} & \text{for 50 kg body weight} \\ \frac{0.157}{\sqrt{t_s}} & \text{for 70 kg body weight} \end{cases} \quad (1.3)$$

where  $t_s$  is the duration of the current exposure in s.

Substituting equations (1.2) and (1.3) in (1.1), the safe step voltage is;

$$V_{step} = (1000 + 6.0C_s(h_s, K)\rho_s) \frac{0.166}{\sqrt{t_s}} \text{ for 50 kg body weight} \quad (1.4a)$$

or

$$V_{step} = (1000 + 6.0C_s(h_s, K)\rho_s) \frac{0.157}{\sqrt{t_s}} \text{ for 70 kg body weight} \quad (1.4b)$$

For safe touch voltage;

$$V_{touch} = (R_B + R_{2Fp})I_B \quad (1.5)$$

where,  $R_{2Fp}$  is the two foot resistances in parallel.

$$\begin{aligned} R_{2Fp} &= 0.5(R_{foot} + R_{Mfoot}) \\ R_{2Fp} &= 1.5C_s(h_s, K)\rho_s \end{aligned} \quad (1.6)$$

Substituting equations (1.6) and (1.3) in (1.5), the safe touch voltage is;

$$V_{touch} = (1000 + 1.5C_s(h_s, K)\rho_s) \frac{0.166}{\sqrt{t_s}} \text{ for 50 kg body weight} \quad (1.7a)$$

$$\text{or, } V_{touch} = (1000 + 1.5C_s(h_s, K)\rho_s) \frac{0.157}{\sqrt{t_s}} \text{ for 70 kg body weight} \quad (1.7b)$$

Fig. (1-2) shows the fibrillating current versus body weight for various animals based on a three second shock [17].

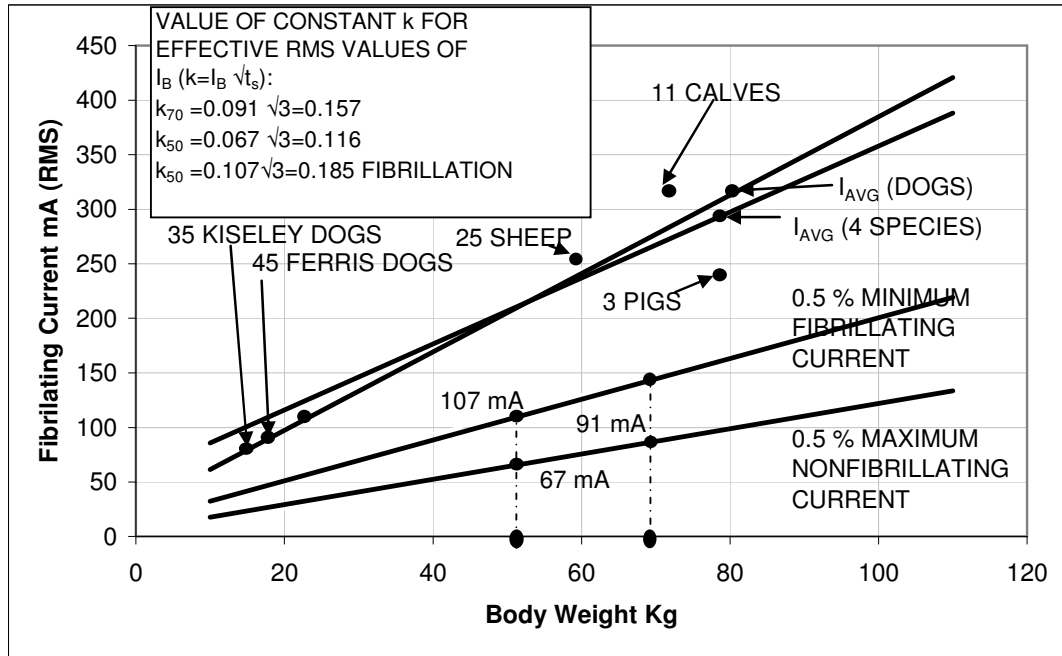


Fig. (1-2) Fibrillating current versus body weight for various animals based on a three second shock [17].

In order to achieve the above condition, some of the basic concepts should be followed;

- 1- The size of grounding system should be large enough to reduce the maximum potential rise when surge current enters it.
- 2- In case of a mesh structure the spacing between the grounding wire should be arranged that the touch and step voltage should be at small value and smaller than safe value for human.
- 3- The downward conductor should be connected to the grounding system at a point in order to reduce the ground potential rise, for example, at the midpoint of the grounding system.
- 4- For inhomogeneous soil, the grounding system should be laid in such a way that it can take advantage of the low resistivity part of the soil to reduce the ground potential rise as much as possible.
- 5- The amount of material for grounding structure should be selected in a way to minimize the cost.

## 1.2 Overview on Earth Surface Potential calculation

Grounding systems play an important part in the design of the extra and ultra high voltage AC substations, plants and some of vital buildings for the purpose of protection from lightning, switching and the faults occur in the system. In this section, methods of Earth Surface Potential (ESP) calculation as derived by various scientists are illustrated.

### 1.2.1 Earth Surface Potential calculation using empirical formulas

In a uniform soil, the quantity grounding resistance ( $R_g$ ) can be calculated with an acceptable accuracy using several simplifying assumptions [17-20]. Touch and step voltages are difficult to calculate by simplified method but it determined by analytical expressions [17].

The ground under the surface of the earth is by no means homogenous, and this makes the analytical analysis of the distributions of currents very difficult if not impossible.

Rüdenberg [17] made an approximation of the vertical rods by dividing it to a large number  $n$  of nearly spherical elements as shown in Fig. (1-3) and he gave an approximation equation to calculate the voltage at certain points on the earth surface due to current pass into vertical electrode which is the following equation,

$$V = \frac{\rho I}{2\pi l} \times \cot \frac{\beta}{2} \quad (1.8)$$

where,  $I$  is the current flows into the rod,  $\rho$  is the resistivity of the soil in  $\Omega.m$ ,  $l$  is the rod length and  $\beta$  is the angle between the axis of the rod and the distance from the rod to the point under consideration at the surface.

Fig. (1-4) illustrates the field strength due to discharge current into rod on the surface around the rod.

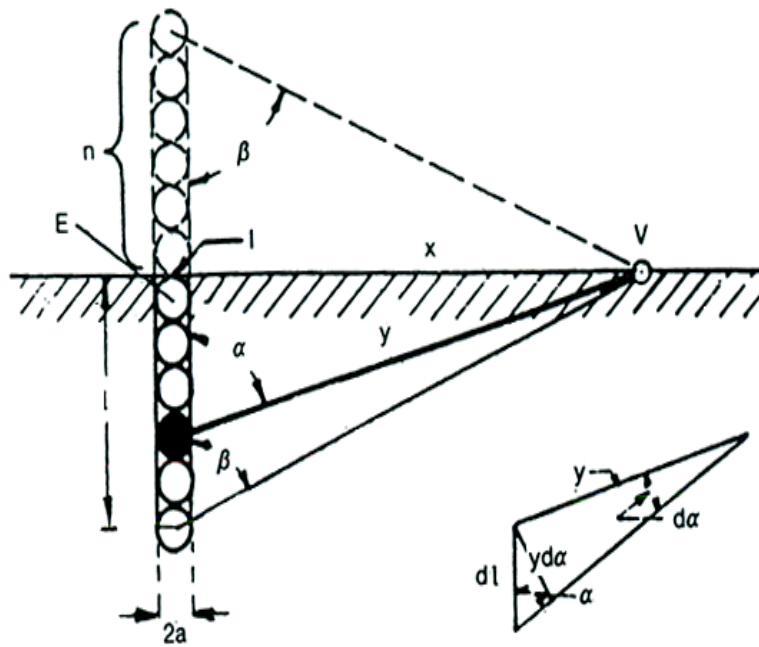


Fig. (1-3) Development of the potential around the rod [17].

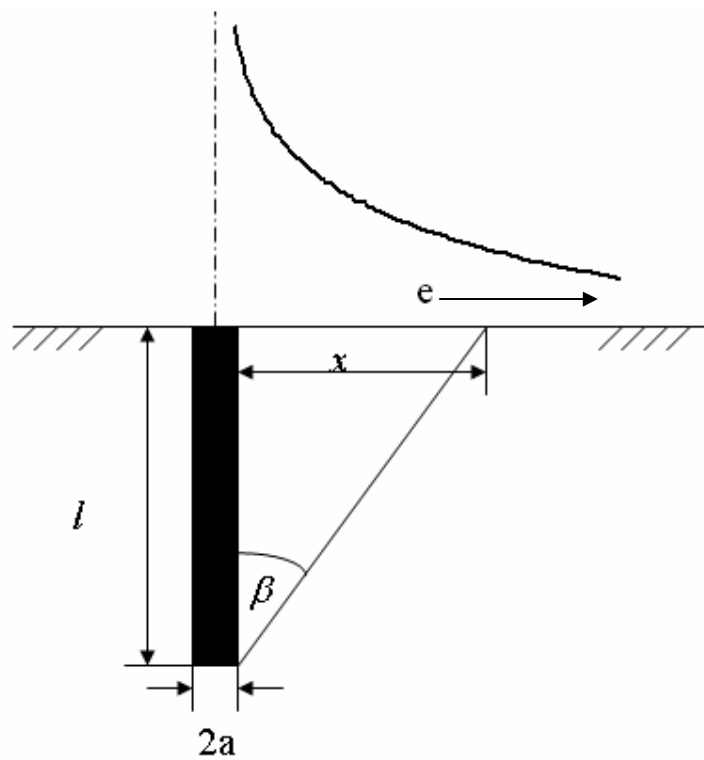


Fig. (1-4) Field strength on the surface around a driven rod [17].

For practical purposes approximation formulas for dangerous voltages, based upon certain simplifying assumptions, have been proposed in [17]. Analytical expressions for mesh and step voltages for a set of parallel conductors have been developed under assumption of uniform current distribution among the grid conductors, omitting the cross connection and conductor end effects [21]. The formulas so obtained have been compared to the results of model tests in electrolytic trough for a sequence of square shaped grounding grids (Fig. (1-5)), reported in [22] and with regard to them the irregularity correction factor (equation (1.13)) has been introduced by Nahman [23], points A, B and C laying on the ground surface above the grounding grid (distance 1m between points B and C). The use of geometrical center A of corner meshes is not rigorously correct as stated in [17], since the point of the lowest potential lies somewhat closer to the perimeter conductors. The mesh and step voltages equations of the ground grid in [17] are,

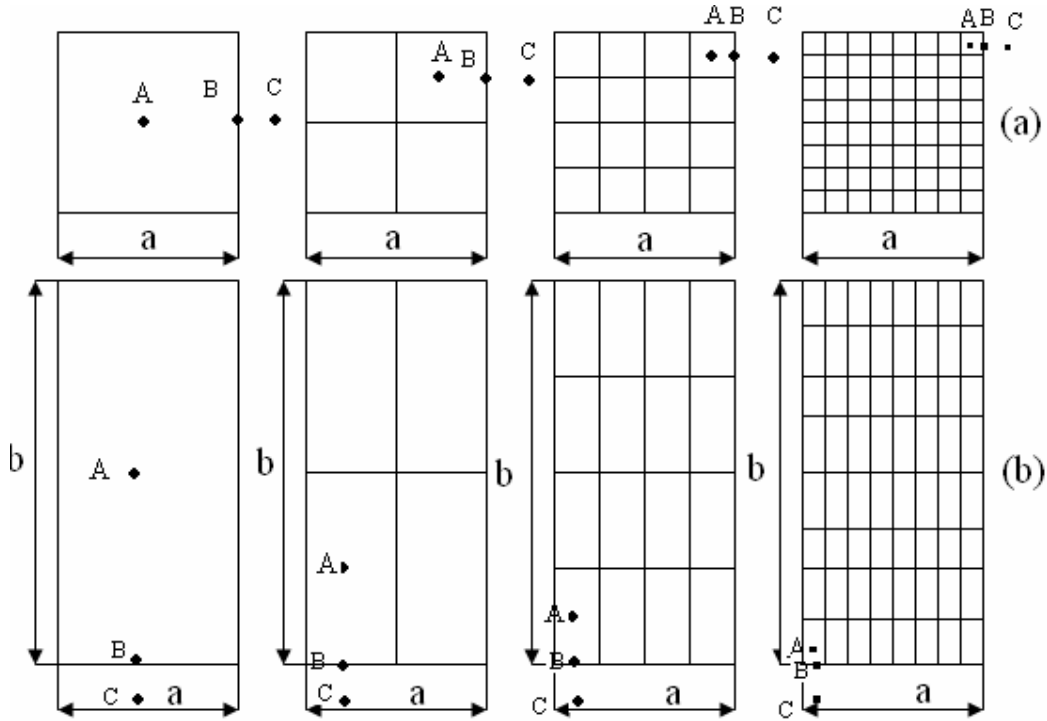


Fig. (1-5) Grounding grids under considerations [23].

$$V_{mesh} = K_m K_{mi} \rho \frac{i_g}{L} \quad (1.9)$$

$$K_m = \frac{1}{2\pi} \ln \frac{D^2}{16hd} + \frac{1}{\pi} \ln \prod_{j=3}^{j=n} \frac{2j-3}{(j-1)^2} \quad (1.10)$$

## Chapter 1: Introduction

where,  $V_{mesh}$  is the maximum touch voltage to be found within a mesh of a ground grid,  $\rho$  is the average soil resistivity in  $\Omega.m$ ,  $i_g$  is the maximum rms current flowing between ground grid and earth,  $L$  is the total length of buried conductors in m, including cross connections, and (optionally) the combined length of ground rods in m,  $K_m$  is the mesh factor defined for  $n$  parallel conductors,  $K_{mi}$  is the irregularity corrective factor for current irregularity,  $h$  is depth in m,  $d$  is the conductor diameter, and  $D$  is space between parallel conductors.

$$V_{step} = K_s K_{si} \rho \frac{i_g}{L} \quad (1.11)$$

$$K_s = \frac{1}{\pi} \left( \frac{1}{2h} + \frac{1}{D+h} + \frac{1}{D} \sum_{j=3}^{j=n} \frac{1}{j-1} \right) \quad (1.12)$$

where,  $V_{step}$  is defined before,  $K_s$  is the step voltage factor and  $K_{si}$  is the irregularity factor of step voltage. The irregularity correction factors  $K_{mi}$  and  $K_{si}$  have the form of a simple linear function of the number of parallel conductors in one direction that is neglecting any cross sections:

$$K_{mi} = K_{si} = 0.172n + C_1 \quad (1.13)$$

Note that Exactly  $C_1=0.656$  since  $K_{mi}$  and  $K_{si}$  must equal 1 for  $n=2$ .

Instead of equation (1.13), as a better approximation of  $K_{si}$  for square grids, and according to the results as in [23] the following formula could be used;

$$K_{si} = 0.083n + 0.65 \quad (1.14)$$

The analysis performed has provided sufficient amount of data for developing more accurate approximate formulas for  $K_{mi}$  and  $K_{si}$  than equations (1.13) and (1.14), involving the influence of various grounding grid parameters.

For square grids the following formula for  $K_{mi}$  has been found

$$K_{mi} = 0.155n + 0.58 + \Delta K_{mi} \quad (1.15)$$

$$\Delta K_{mi} = \begin{cases} 0.155x & , x \leq 16.3 \\ 0.68x - 8.55 & , x > 16.3 \end{cases}$$

$$x = n^3 a^{-1.25} h^{10/a}$$

The factor  $K_{si}$  for square grids can be estimated as

$$K_{si} = (0.069n + 0.556) \left[ 1 + 0.49 \left( \frac{1}{ah^2} - 0.005 \right)^{0.33} \right] \quad (1.16)$$

A simple correlation between the  $K_{mi}$  and  $K_{si}$  parameters of square and rectangular grid has been found.

For the mesh irregularity correction factor of rectangle grids it can be written,

$$K_{mir} = \left[ 0.86 + 0.066(n-2)^{\frac{1}{3}} \right] K_{mi} \quad (1.17)$$

$K_{mi}$  being the mesh factor of square grid with the same  $h$  and  $n$  and  $a$  equal to the longer side of the rectangle grid.

For the step irregularity correction factor of the rectangle grids we have obtained,

$$K_{sir} = \left[ 1 + 0.149 \frac{n}{\sqrt{a}} \right] K_{si} \quad (1.18)$$

$K_{si}$  representing the corresponding factor of square grid with the same  $h$  and  $n$  and  $a$  equal to the shorter side of the rectangle grid.

Nahman concluded that the equation (1.13) that proposed in [17] provides satisfactorily accurate estimations of the mesh voltage irregularity correction factors in all practical cases if the conductor spacing exceeds 5m. The inaccuracies by small spacing increase for greater depths of burial. Separate step voltage irregularity correction factors have to be introduced since they differ significantly from the corresponding mesh voltage factors. The approximation empiric formulas for mesh and step voltage irregularity correction factors are developed, both for square and rectangle grids, involving more completely the effects of various grounding grid parameters. The formulas and charts presented can be of use for practical design purposes.

Dawalibi used a computer program “MALT” that designed to determine grounding performance in uniform and two-layer soil [22]. A variety grounding grid configurations and two layer soil are analyzed in detail. The calculated grounding resistance, step and touch potentials are summarized in [22] which could be used conveniently for practical design purposes. Fig. (1-6) Earth Surface Potential due to various grids in soil model c.

He mentioned that, recently, doubts have been raised about the accuracy of IEEE 80-2000 proposed analytical expressions [17, 23]. The measurements in [24] have been performed with grid models buried at a fixed depth which does not correspond to actual depths as used in practice. Paper [23] have proposed a new expressions for the irregularity factors “ $K_{mi}$ ” and “ $K_{si}$ ” which should prove useful for grounding design in uniform soils. Unfortunately, when the soil is not uniform (almost all grounding systems are installed in non



uniform soils), the pervious expressions for the correction factors are inadequate and can not be used to predict step and touch potentials because the grounding resistances is shown to vary considerably with the degree of heterogeneity of the soil.

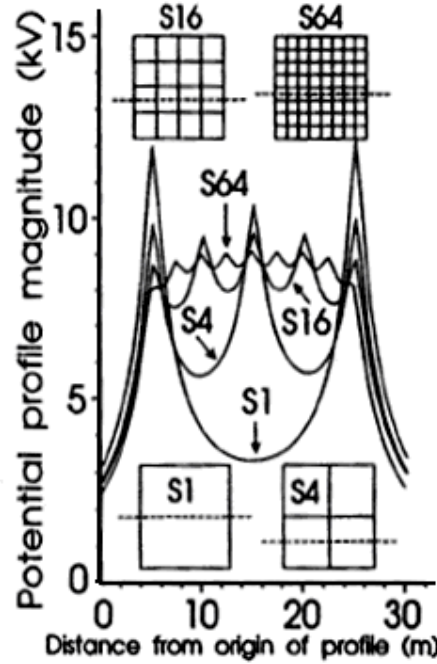


Fig. (1-6) Earth Surface Potential due to various grids in soil model c [22].

Dawalibi proposed another formula for the irregularity correction factor for the mesh voltage which depend on the results that he had gotten, the new expressions for the  $K_{mi}$  is,

$$K_{mi} = \frac{L}{K_m} \frac{V_t \% R}{100 \rho} \quad (1.19)$$

He concluded that the maximum touch potential is not only a function of the grid number of meshes but is also a complex function of the burial grid depth, the top layer height, the reflection factor that present the relation between the resistivities of the two soils.

Another attempt made to improve the IEEE equation for mesh and step voltages by Sverak [21]. It can be stated that the following equation formed the base for all those operations which in the past led to the present simplified formula for  $V_{mesh}$ , equation (1.20):

$$V_{mesh} = V_{my} + V_{mx} = \frac{\rho I}{L} K_i [K_{my}(1,1) + K_{mx}(1,N)] \quad (1.20)$$

where,  $V_{my}$  is vertical component of mesh voltage,  $V_{mx}$  is horizontal component of the mesh voltage and  $N$  is the number of parallel conductors in one direction.

And

$$K_{my}(1,1) = \frac{1}{2\pi} \ln \left[ \frac{4h^2}{4hd - d^2} \right], K_{mx}(1,N) = \frac{1}{2\pi} \sum_{k=0}^{N-1} \ln \left[ \frac{4h^2 + (2k-1)^2 D^2}{4h^2 + 4(kD)^2} \right] \quad (1.21)$$

The modifications of the formulas given in [17] is presented in [25] so that the determination of the mesh and step voltage of a grounding grid which may not be square or rectangle. The results from new formulas are compared with the accurate results obtained from the software program.

Evaluation of maximum step voltages which might appear at the perimeter of a substation site if a ground fault occurs is an important task for a proper substation ground electrode design [26]. Some modifications of available expression for maximum step voltages and associated parameters of ground electrodes buried in uniform soil in order to improve their accuracy and extend their domain of applicability.

### 1.2.2 Earth Surface Potential calculation using numerical methods

Since the early days of the industrial use of the electricity the problem of obtaining the potential distribution produced when a fault current is derived into the ground through a grounding grid has been a challenging one.

Recently, studies based on the Finite-Element Method (FEM) have been used to calculate ground resistance of grounding grids. The first simulation studies of grounding grid behaviour using the FEM were based on calculating ground resistance for an arbitrary grid potential (once the grid current is known). The grid current for the grid potential set is determined by means of a current flow analysis. Once the current is calculated, ground resistance is determined as the quotient between the voltage set and the current calculated [27].

Model size selection was difficult in this method (earth distance to be considered starting from the grounding grid), and this conditioned the value of the calculated ground resistance. To decrease the error of the ground resistance calculated, electrical power engineers were forced to analyze models of different sizes with a high number of nodes. Due to the low levels of accuracy of the results and the long calculation times required, the method is not very feasible. The main problem of the Finite Element Method is that it is necessary to

solve a 3D exterior problem and the Dirichlet boundary condition (the GPR value) must be imposed on the surface of hundreds of electrodes with relation between its length and its diameter is very high. Consequently, the discretization of the domain would be terrible.

A new method to overcome the above difficulties, has been developed that enables ground resistance to be determined starting from the dissipated power or from the stored energy (by the electric field) in the model [28]. This method has the additional advantage of being independent of the boundary condition, shape, and size of the grid and soil structure.

Although the physical phenomena of fault currents dissipation into the earth is a well-known problem that can be modelled by means of Maxwell's Electromagnetic Theory, its application and resolution for the computing of grounding grids of large installations in practical cases present some difficulties. First, it is obvious that no analytical solutions can be obtained in a real case. Moreover, the specific geometry of the grounding systems (a mesh of interconnected bare conductors in which ratio diameter/length is relatively small) precludes the use of standard numerical techniques (such as the Finite Element Method or Finite Differences) since discretization of the domain (the whole ground) is required, and obtaining sufficiently accurate results should imply unacceptable computing efforts in memory storage and CPU time.

For these reasons, during the last years a general numerical formulation based on the Boundary Element Method for the analysis of grounding systems embedded in uniform soil models, which has been successfully applied to real grounding grids have been developed [29, 30]. At present, for real problems, single-layer models ("uniform models") and multilayer models run in real-time in personal computers [31].

Next, a generalization of the BEM formulation for the analysis of grounding systems embedded in stratified soils and the study of the parallelization of that code for its implementation in a high-performance parallel computer is presented. Furthermore, this approach to the analysis of a real grounding system in a layered soil model is applied [29-36].

The behaviour of the electric field in earth generated by a fault current derivation to a grounding grid can adequately be modelled by a Colombian potential that is constant in the grid and its reflected image with respect to the earth's surface. The Extremal Charges Method that allows one to obtain an approximation to the charge distribution as the solution of an optimization problem, specifically a linear programming problem is used [38].

The Extremal Charges Method avoids the troubles associated with the calculus of the auto-influence coefficients that arise in other methods since distinguish between charge

points and evaluation points is taken into account and so all of the coefficients are upperbounded by the inverse of the electrode radius. This fact eliminates the possible numerical instability and, at the same time, keeps the convergence of the approximated solution.

### 1.2.3 Earth Surface Potential calculation using scale model

Another attempts to measure the Earth Surface Potential with the scale model for some different grid configuration is made [39-49]. The approximate formula for the percentage mesh potential given in [40] indicates that if all dimensions of the grid are reduced by the same factor, the percentage mesh potential remains unchanged. The shape of the current and equipotential surfaces is unaltered. Therefore, it is possible to simulate the actual grounding grids with the help of scale models and the potential profiles measured on a model may be used to determine the corresponding potentials on a full scale grid.

A hemispherical water tank with AC voltage source is used in [40, 41], this shape is constructed so that the shape of equipotential surface is nearly identified a free scale reduce model with a real scale model when current flows through the grounding electrode. Fig. (1-7) explain the measurement circuit.

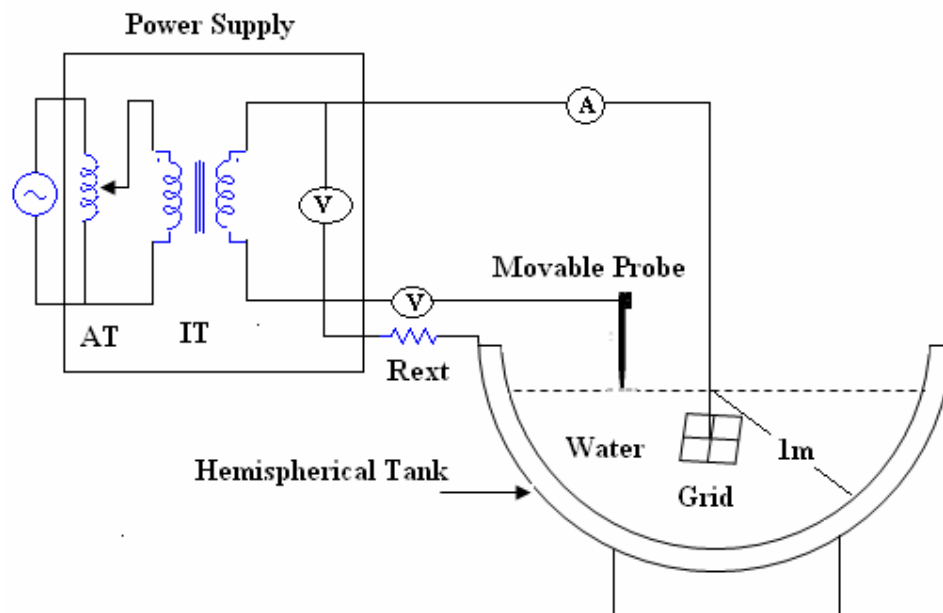


Fig. (1-7) Measurement circuit [41].

As in [17] the factors that affect the transient behaviour of the grounding systems are the shape and dimensions of the grounding system, the soil resistivity of the ground that surrounds the grounding system, the development of soil ionization or not, the injection point and the waveshape of the injected current.

A recent research [42, 43] is made to study the transient behaviour of the grounding grid when the applied impulse current is applied to the grid; the orthogonal tank with the impulse current generator is used as in Fig. (1-8). In [42] the impulse transient impedance by injection the impulse current each time at different point of the grounding grid. In [42] the scale model is used only to reduce the real grid into reduced one but the impulse current shape is not reduced with the same factor and according the similarity theory the scale factor should be taken for all parameters to be able to make a comparison between the behaviour in reality and the behaviour with the model, therefore the front to tail time of the applied impulse wave should be scaled also.

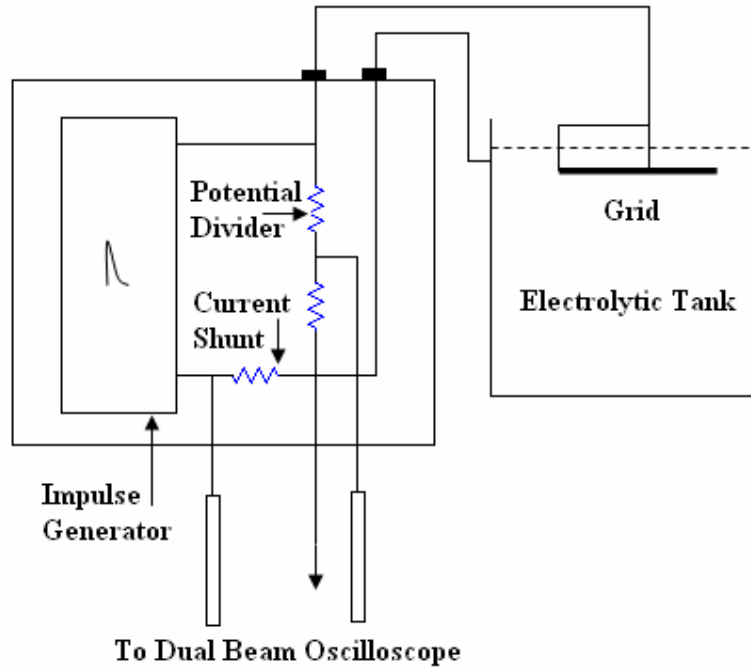


Fig. (1-8) The experimental setup [42].

According to the Similarity Theory, the pervious experimental works lake to scale the time of the impulse waveshape which is very important since the wave propagation for the

## Chapter 1: Introduction

real and scale model should be the same and then the time using with the scale model should be scaled.

The earth surface potential calculation, step and touch voltage with the empirical formulas is convenient for some cases and have a lot of errors and lack accuracy for some other cases since the empirical formulas have a lot of constants and approximations to close its results with the experimental work results.

Therefore, this thesis tries to carry out some experimental works to study the transient behavior of grounding grid subjected to lightning taking into account the scaling time issue, as well as a more accurate and practical method is used to calculate the Earth Surface Potential above the grounding grid during the abnormal conditions and also improve the grounding grid design using Evolutionary Strategies.



## Chapter 2

### Terminology and Definitions

The operation of grounding systems is a topic which has been extensively studied and analyzed in the last four decades, and several methods for grounding analysis and design have been proposed. Furthermore, several computer programs have been developed to calculate the safety parameters of grounding installation in order to obtain a reliable model of the grounding system and the hazardous scenarios which could occur. Most of these methods are based on the professional experience, on semi-empirical works, on experimental data obtained from scale model assays and laboratory tests, or on intuitive ideas. Unquestionably, these contributions represented an important improvement in the grounding analysis area, although some problems have been systematically reported, such as the large computational costs required in the analysis of real cases, the unrealistic results obtained when segmentation of conductors is increased, and the uncertainty in the margin of error [17, 36, 52, 53].

The phenomenon that accompanied with the lightning stroke are the potential rise, the potential difference and transient energy transfer between grounding system and the external world (other structures located in the vicinity), if the grounding system is inadequate for avoiding these phenomenon, great risks may be occur to the equipments and human. For transmission line towers, the guard wires consider the primary defense from the lightning stroke. When the lightning stroke strikes the guard wire and the grounding system is inadequate design (ground resistance “ $R_g$ ” has high value), the potential rise on it and the potential difference develops between the guard wire and the power transmission line, and hence the flashover occurs between them and may be great risks occur. Also, some structures must obey to great safety conditions such as buildings that use for reserving flammable and explosive materials, the grounding system becomes very important, the lack of good grounding may be help for explosion if the lightning strikes the buildings of near from it.

### 2.1 Definitions

- A grounding system is a metallic structure that is buried in the soil. It may be realised as single horizontal wire, vertical rod, grounding grid (a complicated configuration for grounding system) and some of combination between the pervious aspects. The grounding system creates an easy path to current that is caused by lightning or by switching. The grounding resistance ( $R_g$ ) is the resistance between the grounding gird and the remote earth.



- The touch voltage ( $V_t$ ) is the difference between the ground potential rise (GPR) and the surface potential at the point where a person is standing while at the same time having his hands in contact with a grounded structure.
- The mesh voltage is defined as the maximum touch voltage to be found within a mesh of a ground grid.
- The transferred voltage (ground potential rise GPR) is the product of the grounding grid resistance and the fault current ( $I_f$ ).
- The maximum touch voltage is the difference between the GPR and the lowest potential in the grid boundary [17]. The maximum percentage value of  $V_{touch} \%$  is given by [37, 54, 55];

$$V_{touch} \% = \frac{GPR - V_{min}}{GPR} \times 100 \quad (2.1)$$

where, GPR is the product of the fault current and grounding resistance and  $V_{min}$  is the minimum surface potential in the grid boundary.

- The step voltage ( $V_s$ ) is the difference in surface potential experienced by a person bridging a distance of 1 m with his feet without contacting any other grounded object [17].
- The maximum step voltage of a grid will be the highest value of step voltages of the grounding grid. The maximum step voltage can be calculated by using the slope of the secant line.
- Profile location is the number of points on the earth surface that the voltage is desired, and helps us to know the voltage that the man affects.
- Similarity theory is closely related and is used in experiments with models. If the similarity conditions are fulfilled, it is necessary to know the scale factors for all the corresponding quantities in order to calculate all the characteristics in nature from data on the dimensional characteristics in the model.

Fig. (2-1) explains the touch voltage, step voltage, mesh voltage and transferred voltage.

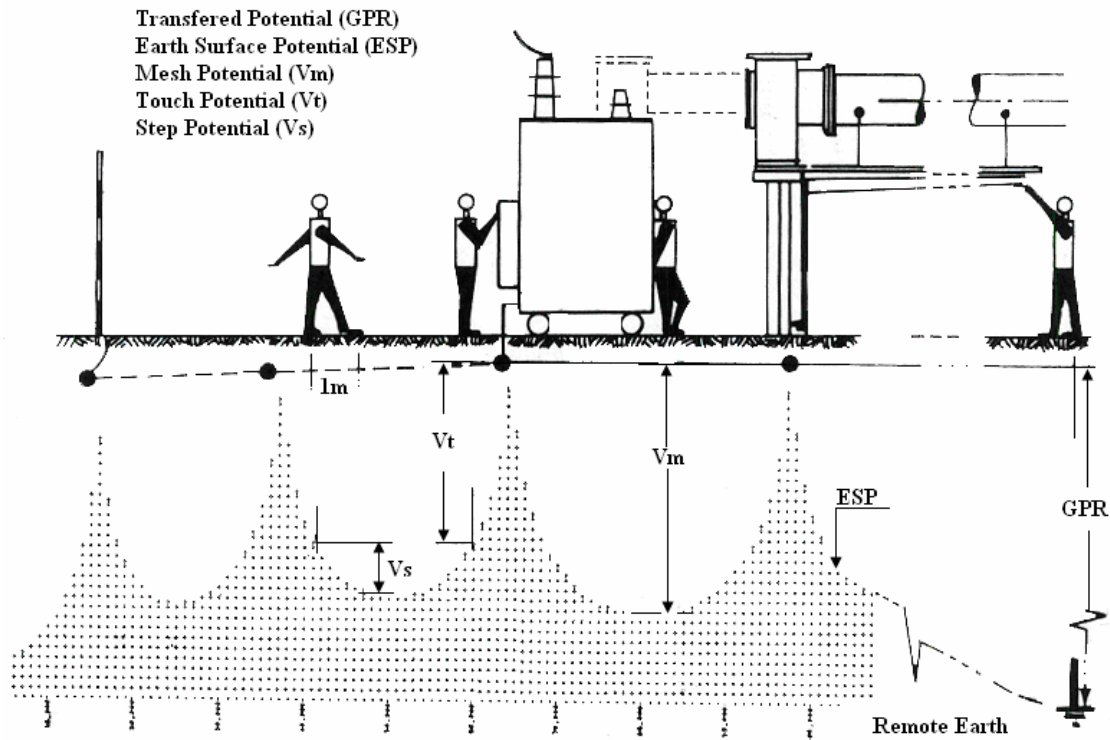


Fig. (2-1) Illustration of the touch and step voltages for grounding grids [17].

- Evolution Strategy (ES, from German *Evolutionsstrategie*) is an optimization technique based on ideas of adaptation and evolution.
- Optimization, or mathematical programming, refers to the study of problems in which one seeks to minimize or maximize a real function by systematically choosing the values of real or integer variables from within an allowed set.
- Evolutionary Algorithm (EA) is a subset of evolutionary computation, a generic population-based metaheuristic optimization algorithm. An EA uses some mechanisms inspired by biological evolution: reproduction, mutation, recombination, natural selection and survival of the fittest. Candidate solutions to the optimization problem play the role of individuals in a population, and the cost function determines the environment within which the solutions "live".
- Quality is defined as the totality of characteristics of a product or service that bears on its ability to satisfy stated and implied needs and also the result of a comparison between what was required and what was provided.



# Chapter 3

## Experimental Investigations

As the number and complexity of AC substations increase, the need for accurate design procedures for the grounding system becomes more important both from a safety point of view and from financial considerations. The analytical techniques used have varied from those using simple hand calculations to those involving scale models to sophisticated digital computer programs.

The technique of using scale models in an electrolytic tank to determine the surface potential distribution during ground faults was introduced in a paper [39-50].

The calculation of Earth Surface Potential using scale models should be made after understanding the Similarity Theory. It has been widely applied in aeromechanics, hydrodynamics, problems of explosion and astrophysical problems [51].

Dimensional analysis and Similarity Theory are closely related and are used in experiments with models. In such experiments, one replaces the investigation of a phenomenon in nature by the investigation of an analogous phenomenon in a model of smaller or larger scale (usually under special laboratory conditions). If the similarity conditions are fulfilled, it is necessary to know the scale factors for all the corresponding quantities in order to calculate all the characteristics in nature from data on the dimensional characteristics in the model.

The goal of the experimental work using scale model is to know something about the behavior of the grid structure, i.e. is there a transient behavior that needs complex models or is a static model sufficient.

### 3.1 Scale model with scaling time of the applied impulse current

Many efforts are done to calculate the Earth Surface Potential due to charging current into grounding grid by scale mode using electrolytic tank as mentioned before. The scale factor is assumed to convert the dimensions of the real grounding grid to the corresponding in the model. The scaling of the time of the applied impulse is very important according to the similarity theory and also according to the wave propagation in the conductors of the grid. A simple formula for the wavelength is as the follow:

$$\lambda = \frac{v}{f} \quad (3.1)$$

Where,  $\lambda$  is wavelength,  $v$  is the velocity of propagation and  $f$  is the frequency of the signal or the impulse.

Then if the length of the conductor is  $\lambda_1$  and the impulse frequency is  $f_1$  as in reality and if the length of the conductor is reduced as a model to  $\lambda_2$  by a specified scale factor, since the velocity of propagation must be constant, then the impulse frequency applied to the model should be increased by the same scale factor, this means the corresponding time of the waveshape of the impulse which applied to the model is reduced by the same scale factor.

The very important issue now how to reduce the front to tail time of the proposed waveshape from 7/30  $\mu s$  (the waveshape of the surge impulse current from the impulse generator depend on the load resistance which is the grounding grid resistance in this case) to 70/300  $ns$ , this means that we take scale factor 100. Since only an impulse generator for producing a surge impulse (open circuit voltage 1.2/50  $\mu s$ , short circuit current 8/20  $\mu s$ ) was available, an additional pulse forming network is realized. The network has been modeled and optimized with the network calculation tool “SPICE”. Fig. (3-1) shows the pulse forming network and the  $S_1$  refer to the surge arrester,  $R_g$  to the grounding grid resistance. The result of the waveform produced with the scaled time in shown in Figs. (3-2) and (3-3), show the waveforms of the impulse current when using surge generator with pulse forming network.

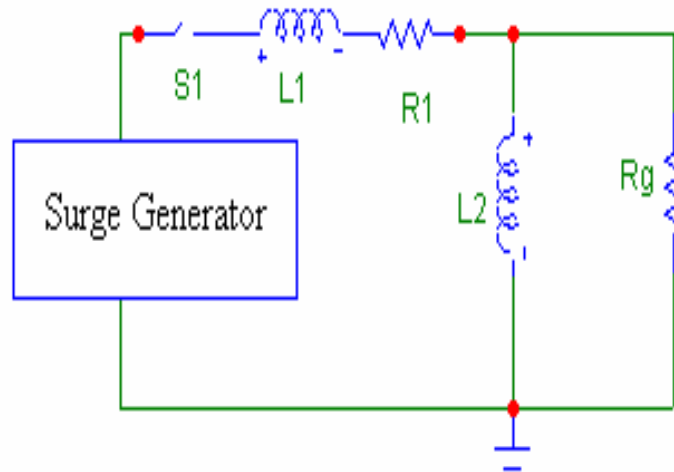


Fig. (3-1) Schematic diagram for time scaling circuit.

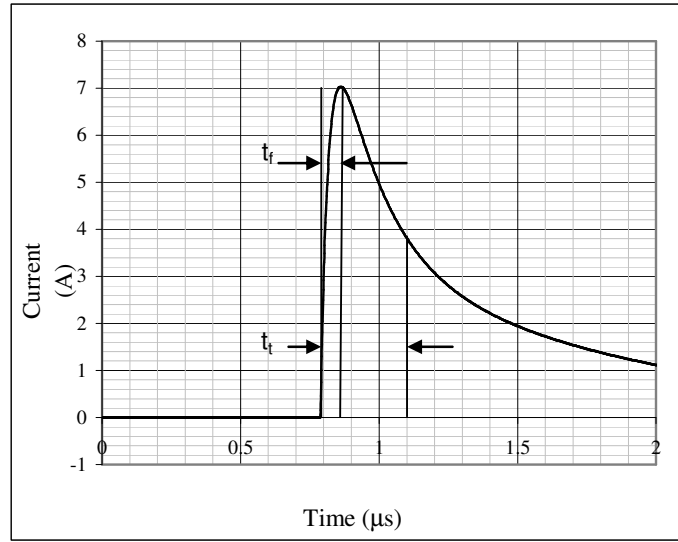


Fig. (3-2) The waveform of the applied current with the proposed front to tail time  $t_f/t_t=70/300$  ns.

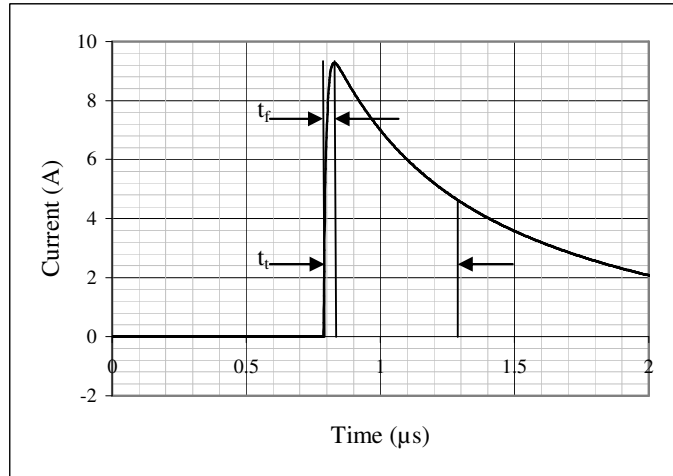


Fig. (3-3) The impulse form at 12/500 ns.

## 3.2 Test setup

The approximate formula for the percentage mesh potential given in [40] indicates that if all dimensions of the grid are reduced by the same factor, the percentage mesh potential remains unchanged. The shape of current and equipotential surfaces is unaltered, but the time also has to be scaled. Therefore, it is possible to simulate the actual grounding grids with the help of scale models and the potential profiles measured on a model may be used to determine the corresponding potentials on a full scale grid.

Although the best shape for an electrolytic tank is hemispherical, cylindrical or orthogonal, the latter is more often used [42, 43]. The dimensions of the electrolytic tank which has been used for the experiment are  $2.0 \times 1.0 \times 0.48 \text{ m}^3$ .

For a scale factor 100:1, a 16 mesh grid with outside dimensions of  $50 \times 50 \text{ cm}^2$  have been modelled and tested. The rise to tail time is reduced also by this factor and this is very important issue according to the theory of similarity. The rise to tail time is modelled as  $70/300 \text{ ns}$  and this corresponds to  $7/30 \text{ } \mu\text{s}$  which act in reality as impulse wave-shape. The depth of the tank must not be less than half the side of the tank. Salted tap water is used as an electrolyte, which serves as an adequately conducting medium, representing the homogeneous earth. Change in the salinity causes a change in the liquid resistivity.

The layout of the grounding grid as in Fig. (3-8) is tested experimentally under the above mentioned impulse. The grid was placed in the centre of the full water tank, and at depth of 2.5 cm under the water surface. The model grid was hung on nylon fishing lines below the surface of the electrolyte. Hanging provides a horizontal configuration with minimum deformation and bend.

The characteristics of the grid are  $50 \times 50 \text{ cm}^2$ , the radius of the grid rods ( $r$ ) is 8 mm, the grid depth ( $h$ ) is 2.5 cm, and the conductivity of the water ( $\sigma$ ) is  $1600 \text{ } \mu\text{S/cm}$ .

The injection of the current was applied to the corner of the grid. Due to the grids' symmetries, measurements were not conducted at all points, but some points outside the boundary of the grid because the slope is large and then the difference between the measured points may be significant.

The components of the test setup are;

1. Electrolytic tank which simulates the homogenous earth with dimensions 200cm long, 100cm wide, 48cm high and the conductivity of the salty water is  $1600 \text{ } \mu\text{S/cm}$ , Fig. (3-4a, b).
2. Ultra compact Impulse generator (EM test- UCS 500-M), able to deliver a surge (hybrid) impulse (open circuit up to 4kV, impulse form  $1.2/50 \mu\text{s}$ , short circuit current up to 2kA, impulse form  $8/20 \mu\text{s}$ , Fig. (3-5).
3. Oscilloscope type Tektronix -DPO4014, bandwidth 1 GHz, sample range up to 5 GS/s on all channels, 4 channel model, Fig. (3-6).
4. Conductivity measurements were performed with a WTW Microprocessor Conductivity meter type LF2000, Fig. (3-7).
5. The current probe type Tektronix P6021- 60 MHz is used.

6. Grid: with 16 meshes, 50\*50cm long, and radius 10mm, Fig. (3-8).
7. Pulse forming network that is used to reduce the time of the impulse wave shape by factor 100, Fig. (3-9).



Fig. (3-4a) The Electrolytic tank with water, grid and probs.



Fig. (3-4b) The Electrolytic tank with grid.





Fig. (3-5) Ultra compact Impulse generator.



Fig. (3-6) Oscilloscope type Tektronix -DPO4014.



Fig. (3-7) WTW Microprocessor Conductivity meter type LF2000.

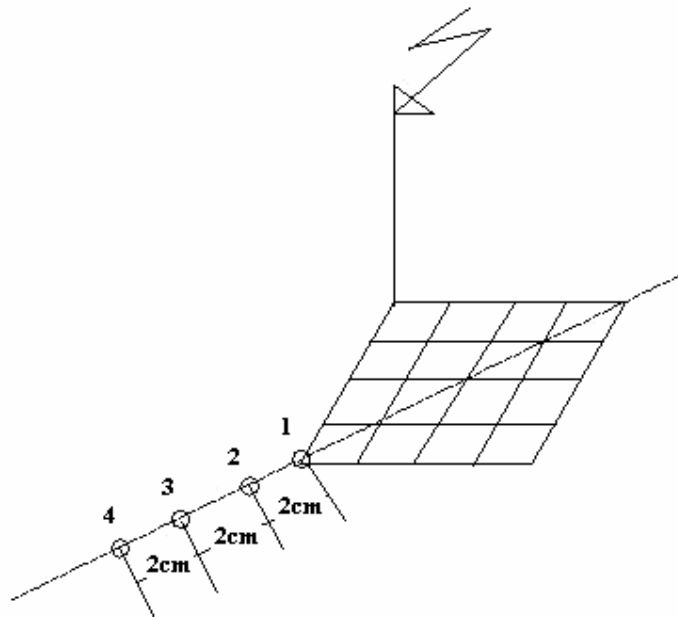


Fig. (3-8) Configuration of grid that used as scale model.



Fig. (3-9) Scale time circuit.

### 3.3 Test results

In the beginning of the experiment, some difficulties are experienced to measure the voltage of specified points on the water surface.

The first one is the return current experiences high inductive load of the metal sheet which was used as return current path. The magnetic field produced in this loop induced a significant signal into the measurement system.

Also we can not consider the metal sheet as reference voltage and hence, it is difficult to determine the voltage at the points on the water surface. To overcome this difficulty, a copper conductor is connected between the upper and lower metal sheet to decrease the inductive effect and measured the voltage difference between two points on the water surface, which makes the reference point superfluous. The solution is shown as in Figs. (3-10) and (3-11).

The second difficulty is that, the impulse has a very fast rise time, which produces an electromagnetic wave, which is radiated from the wires. The electromagnetic pulse disturbs the measurement signal directly through the housing of the oscilloscope. A metallic shield is shown as in Fig. (3-12), in which the oscilloscope has been located, reduce this effect significantly.



Fig. (3-10) The probe used to measure the voltage difference between two points on the water surface.



Fig. (3-11) Reduction the length return current path.



Fig. (3-12) Elimination of the interference from external signal sources using metal housing.

After overcoming these difficulties, the measurements were done by measuring the voltage difference between two points 2cm apart from outside corner mesh of the grid along the diagonal profile as in Fig. (3-8). The setting of the current probe is 10 mA/1 mV. The average between two measurements with changing the polarity of the probe is calculated. The results are shown in the Figs. 3-13a, 13b, 14a, 14b, 15a, 15b and in table (3-1). Table (3-1) shows the voltage differences between each of two points as in Fig. (3-8).

It is observed from Figs3-13a, 13b, 14a, 14b, 15a, 15b that no oscillations appear in the current and voltage difference waveforms. This is considered very important conclusion because the transient behaviour of the grounding system can be neglected and therefore, the static model is sufficient to simulate the transient behaviour.

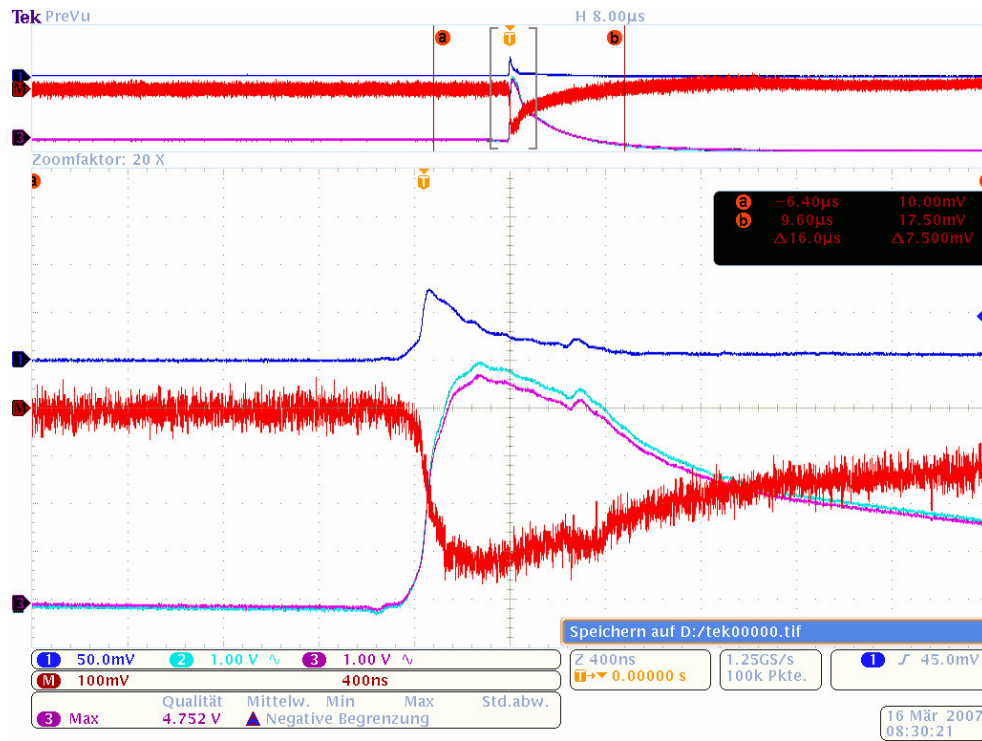


Fig. (3-13a) Current (0.5 A/div) and the voltage difference (100 mV/div) between points 1 and 2 as in Fig. (3-8).

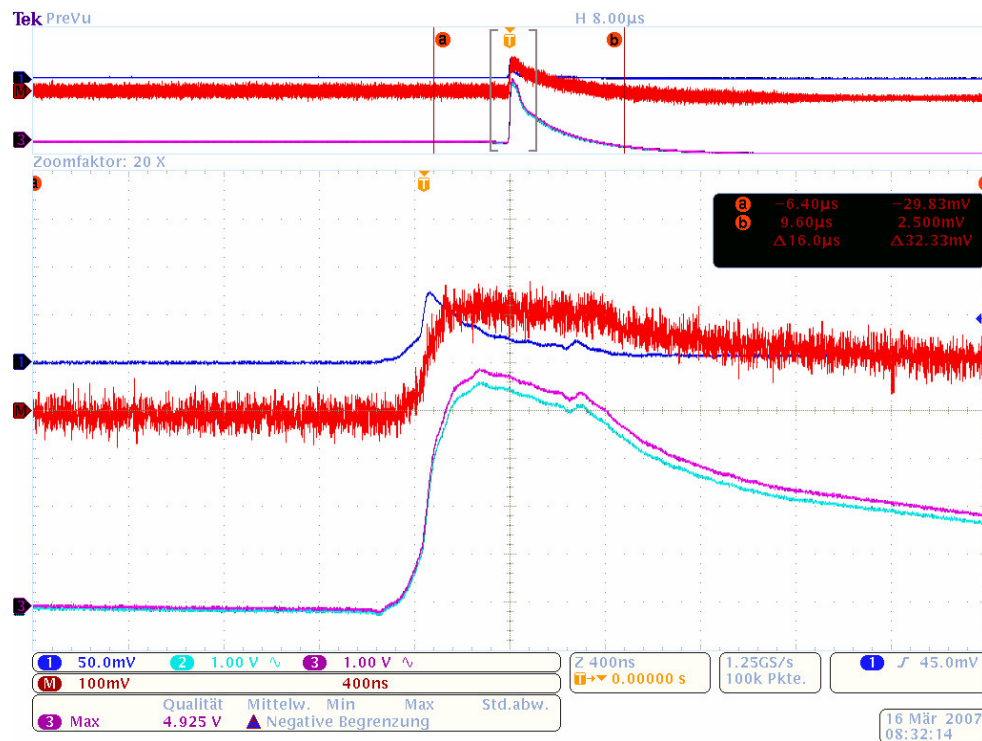


Fig. (3-13b) Current (0.5 A/div) and the voltage difference (100 mV/div) between points 1 and 2 as in Fig. (3-8) when changing the polarity of the voltage probe.



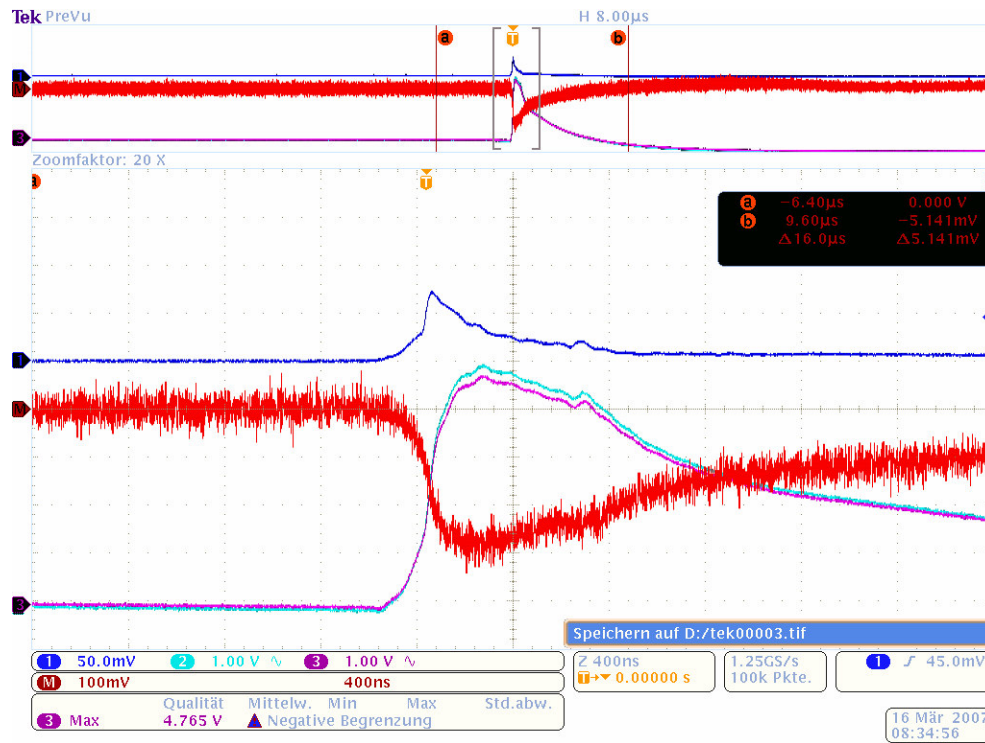


Fig. (3-14a) Current (0.5 A/div) and the voltage difference (100 mV/div) between points 2 and 3 as in Fig. (3-8).

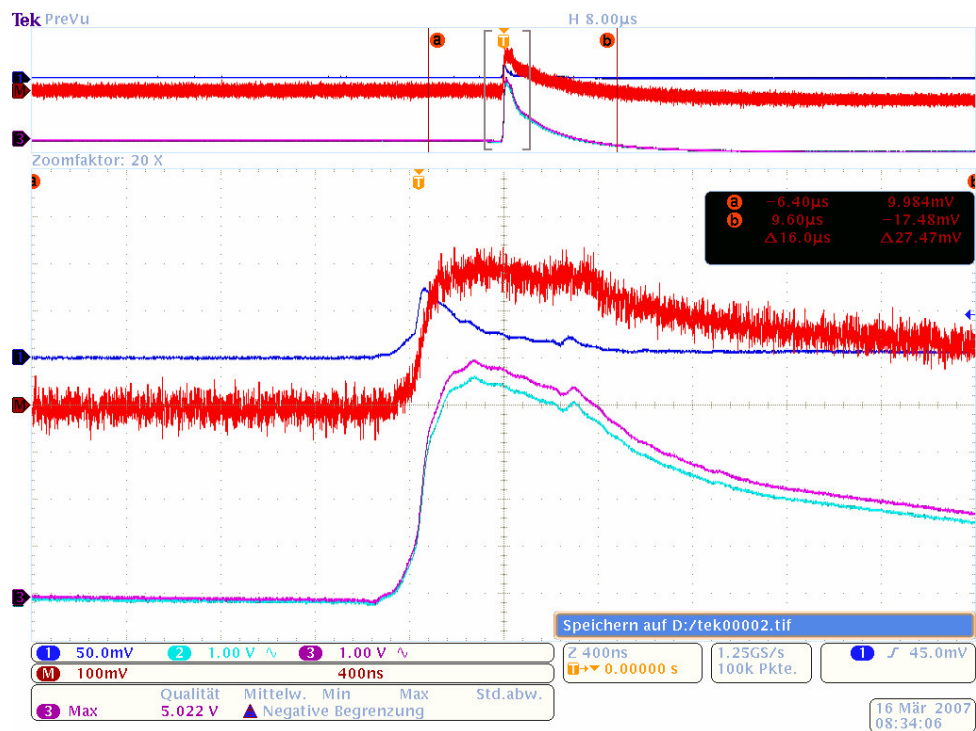


Fig. (3-14b) Current (0.5 A/div) and the voltage difference (100 mV/div) between points 2 and 3 as in Fig. (3-8) when changing the polarity of the voltage probe.

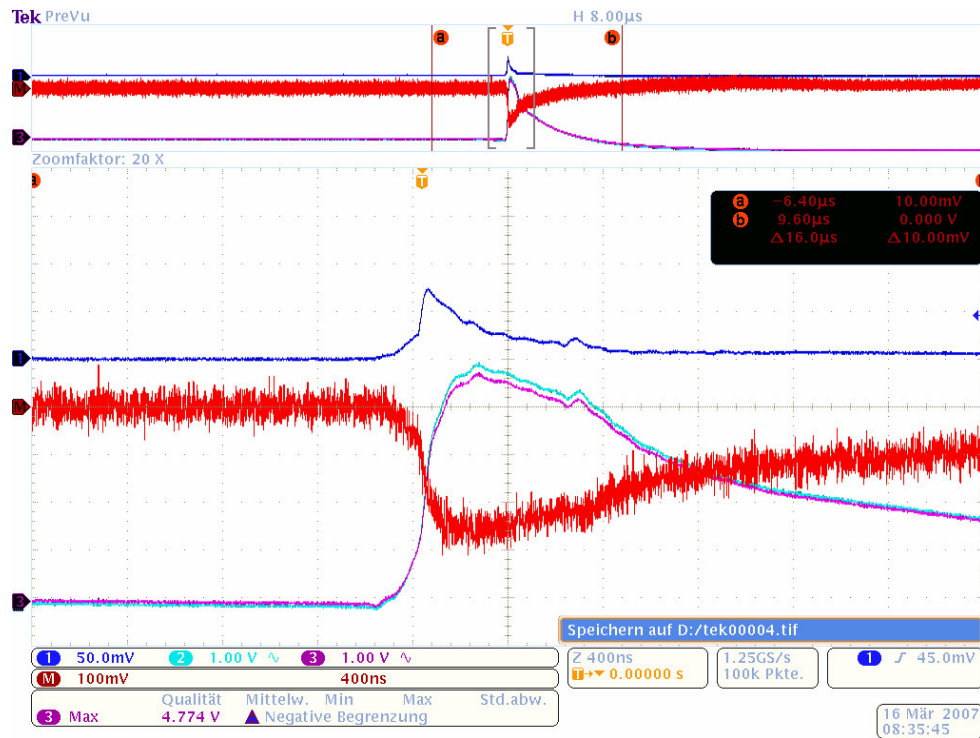


Fig. (3-15a) Current (0.5 A/div) and the voltage difference (100 mV/div) between points 3 and 4 as in Fig. (3-8).

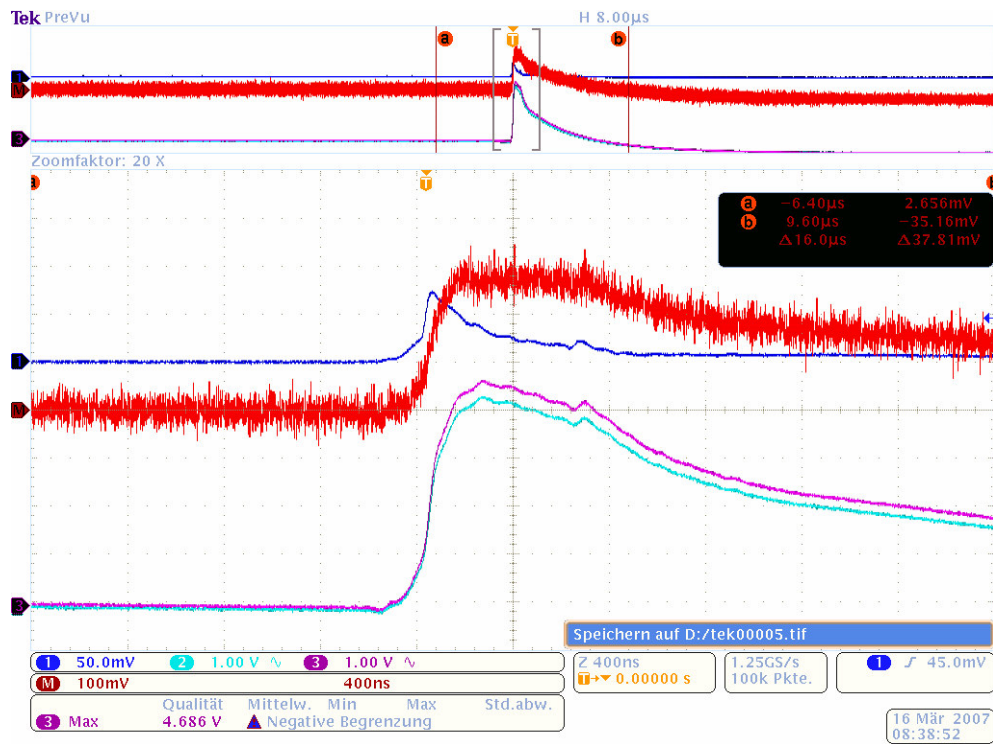


Fig. (3-15b) Current (0.5 A/div) and the voltage difference (100 mV/div) between points 3 and 4 as in Fig. (3-8) when changing the polarity of the voltage probe.



Voltage difference from the Figs. (3-13a, 13b, 14a, 14b, 15a, 15b) at Peak current 0.75 A.					
$V_{12}$ (mV)	370	$V_{23}$ (mV)	300	$V_{34}$ (mV)	290
$V_{21}$ (mV)	250	$V_{32}$ (mV)	300	$V_{43}$ (mV)	310
$V_{ave}$ (mV)	310	$V_{ave}$ (mV)	300	$V_{ave}$ (mV)	300

Table (3-1) The average values of the measured voltage at specified points as in Fig. (3-8).



# Chapter 4

## Methods of Calculation

The experimental work using scale model in the previous chapter explains that no oscillations appear in the current and voltage difference waveforms. One can conclude from this observation that the transient behaviour of the grounding system can be neglected for typical lightning impulse waveforms and therefore, the static model is sufficient to simulate the transient behaviour. In this chapter, two methods to calculate the Earth Surface Potential due to discharging impulse current into grounding grid are presented, one is the Boundary Element Method and the other is Charge Simulation Method.

In many fields of scientific and engineering computing, it is necessary to solve boundary values problems of partial differential equations over unbounded domains. For this kind of problems, the standard techniques such as the Finite Element Method (FEM), which is effective for most problems over bounded domain, will meet some difficulties and the corresponding computing cost will be very high. The advantage of the BEM is the reduction of the problem dimension: only the boundary of the sound-radiating structure must be discretized. The cost of preprocessing and mesh generation is thus greatly reduced.

Charge Simulation Method (CSM) has been recognized to be very competitive and often superior to FEM or FDM, at least for treating two- or three-dimensional fields within H.V. insulation systems, particularly where high accuracies within highly divergent field areas are demanded. The attractiveness of this method which uses when compared with the Finite Element and Finite Difference Method emanates from its simplicity in representing the equipotential surfaces of the electrodes, its application to unbounded arrangements whose boundaries extend to infinity and its direct determination to the electric field.

### 4.1 Boundary Element Method

The Boundary Element Method is a numerical computational method of solving linear partial differential equations which have been formulated as integral equations (i.e. in boundary integral form). It can be applied in many areas of engineering and science including fluid mechanics, acoustics, electromagnetics, and fracture mechanics. (In electromagnetics, the more traditional term "method of moments" is often, though not always, synonymous with "Boundary Element Method".) The integral equation may be regarded as an exact solution of the governing partial differential equation.

The Boundary Element Method attempts to use the given boundary conditions to fit boundary values into the integral equation, rather than values throughout the space defined by a partial differential equation. Once this is done, in the post-processing stage, the integral equation can then be used again to calculate numerically the solution directly at any desired point in the interior of the solution domain. The Boundary Element Method is often more efficient than other methods, including finite elements, in terms of computational resources for problems where there is a small surface/volume ratio. Conceptually, it works by constructing a "mesh" over the modelled surface.

BEM is applicable to problems for which green's functions can be calculated. These usually involve fields in linear homogeneous media. This places considerable restrictions on the range and generality of problems to which boundary elements can usefully be applied. Nonlinearities can be included in the formulation, although they will generally introduce volume integrals which then require the volume to be discretised before solution can be attempted, removing one of the most often cited advantages of BEM. A useful technique for treating the volume integral without discretising the volume is the dual-reciprocity method. The technique approximates part of the integrand using radial basis functions (local interpolating functions) and converts the volume integral into boundary integral after collocating at selected points distributed throughout the volume domain (including the boundary). In the dual-reciprocity BEM, although there is no need to discretise the volume into meshes, unknowns at chosen points inside the solution domain is involved in the linear algebraic equations approximating the problem being considered.

The green's function elements connecting pairs of source and field patches defined by the mesh form a matrix, which is solved numerically. Unless the green's function is well behaved, at least for pairs of patches near each other, the green's function must be integrated over either or both the source patch and the field patch. The form of the method in which the integrals over the source and field patches are the same is called "Galerkin's method". Galerkin's method is the obvious approach for problems which are symmetrical with respect to exchanging the source and field points. In frequency domain electromagnetics this is assured by reciprocity. The cost of computation involved in naive Galerkin implementations is very severe. One must loop over elements twice (so we get  $n$ -squared passes through) and for each pair of elements we loop through gauss points in the elements producing a multiplicative factor proportional to the number of gauss-points squared. Also, the function evaluations required are typically quite expensive, involving trigonometric/hyperbolic

function calls. Nonetheless, the principle source of the computational cost is this double-loop over elements producing a fully populated matrix.

The Green's functions, or fundamental solutions, are often problematic to integrate as they are based on a solution of the system equations subject to a singularity load (e.g. the electrical field arising from a point charge). Integrating such singular fields is not easy. For simple element geometries (e.g. planar triangles) analytical integration can be used. For more general elements, it is possible to design purely numerical schemes that adapt to the singularity, but at great computational cost. Of course, when source point and target element (where the integration is done) are far-apart, matters are very straight-forward and it is possible to integrate very easily due to the smooth decay of the fundamental solution. It is this feature that is typically employed in schemes designed to accelerate/compress boundary element problem calculations.

In the last decades, some intuitive techniques for grounding grid analysis such as the Average Potential Method (APM) have been developed. A new Boundary Element Approach has been recently presented [29-36] that includes the above mentioned intuitive techniques as particular cases. In this kind of formulation the unknown quantity is the leakage current density, while the potential at an arbitrary point and the equivalent resistance for grounding grids must be computed subsequently.

A Boundary Element Method software package (TOTBEM) is used to get the numerical computation of grounding system analysis such as the equivalent resistance and the distribution of potential on the earth surface due to fault currents.

## 4.2 Charge Simulation Method

In the Charge Simulation Method, the actual electric field is simulated with a field formed by a number of discrete charges which are placed outside the region where the field solution is desired. Values of the discrete charges are determined by satisfying the boundary conditions at a selected number of contour points. These contour points have the same voltage  $V$ . Once the values and positions of simulation charges are known, the potential and field distribution anywhere in the region can be computed easily [56].

The basic principle of the Charge Simulation Method is very simple. If several discrete charges of any type (point, line, or ring, for instance) are present in a region, the electrostatic potential at any point  $C$  can be found by summation of the potentials resulting from the individual charges as long as the point  $C$  does not reside on any one of the charges. Let  $Q_j$  be

a number of  $n$  individual charges and  $\Phi_i$  be the potential at any point  $C$  within the space. According to superposition principle

$$\phi_i = \sum_{j=1}^n P_{ij} Q_j \quad (4.1)$$

where  $P_{ij}$  are the potential coefficients which can be evaluated analytically for many types of charges by solving Maxwell equations,  $\Phi_i$  is the potential at contour (evaluation) points,  $Q_j$  is the charge at the point charges.

As in Fig. (4-1), the fictitious charges are taken into account in the simulation as point charges. Equal number of the point charges placed on the axial of each conductor in the grid. Because of the ground surface is flat, the method of images can be used with the Charge Simulation Method and the potential will be characterized for being constant on the grounding grids and its symmetry [37, 38]. The potential coefficients  $P_{ij}$  will be as in the following equation;

$$P_{ij} = \frac{1}{4\pi\epsilon} \left[ \frac{1}{d_{ij}} + \frac{1}{d'_{ij}} \right] \quad (4.2)$$

where,  $d_{ij}$  is the distance between contour point  $i$  and charge point  $j$  and  $d'_{ij}$  is the distance between the contour point  $i$  and image charge point  $j'$  as shown in Fig. (4-1).

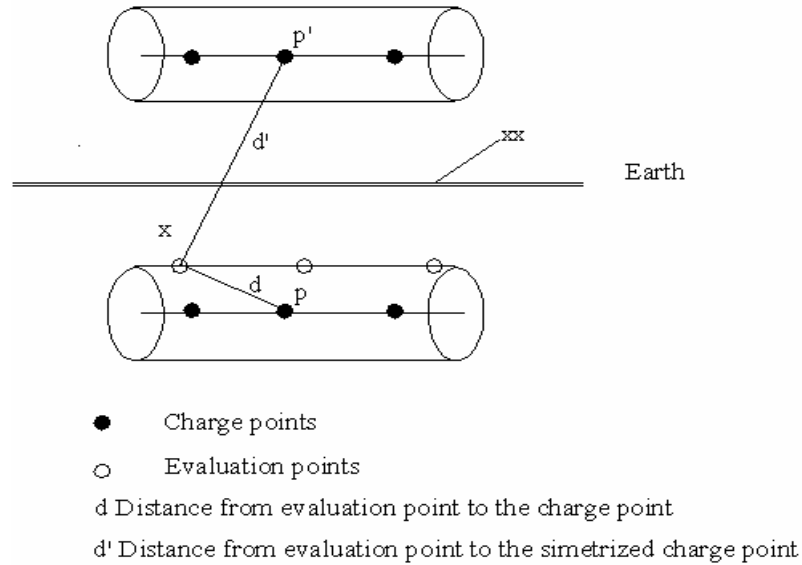


Fig. (4-1) Illustration of CSM.

The position of each point charges and each contour point are determined in X, Y and Z coordinates where the distance between the contour (evaluation) points are calculated as the following ;

$$d_{ij} = \sqrt{(X_j - X_i)^2 + (Y_j - Y_i)^2 + (Z_j - Z_i)^2} \quad (4.3)$$

where,  $X_j$ ,  $Y_j$  and  $Z_j$  are the coordinates of the point charge and  $X_i$ ,  $Y_i$  and  $Z_i$  are the coordinates of the contour point.

$P_{ij}$  constitute the potential coefficient matrix and to get the unknown charge  $Q_j$  when the voltage at the contour points  $i$  is known and equal to  $V$  volt, the inverse matrix for  $P_{ij}$  should be calculated. Because of the large number of assumed point charges, a suitable method to get the inverse matrix should be chosen.

Since both the Gaussian elimination and Gauss-Jordan elimination share the disadvantage that all right hand sides must be known in advance. The proposed method LU Decomposition method does not share this deficiency, and also has an equally small operations count, both for the solution with any number of right hand sides, and for matrix inversion. Therefore, the suitable method to get the inverse matrix for  $P_{ij}$  is the LU Decomposition [57].

After solving equations (4.1) by knowing the inverse matrix of  $P_{ij}$ , the magnitude of simulation charges is determined, as soon as an adequate charge system has been developed, the potential and field at any point  $xx$  outside the electrodes can be calculated again by using the following equation;

$$\phi_{xx} = \sum_{j=1}^n P_{xxj} Q_j \quad (4.4)$$

where,  $\phi_{xx}$  is the voltage at the arbitrary point  $xx$ ,  $P_{xxj}$  is the potential coefficient matrix for the point  $xx$  with all point charges and  $Q_j$  is the calculated point charges.

A number of checked points located on the electrodes where potentials are known as  $V$ , are taken to determine the simulation accuracy.

The basic design quantities of the grounding grids are the ground resistance ( $R_g$ ), the ground potential rise (GPR), touch and step voltages as showed in Fig. (2-1), these pervious quantities depend on the grid parameters, which are the side lengths of it, radius of grid conductors and length of vertical rods.

The Charge Simulation Method is used to get the ground resistance ( $R_g$ ), ground potential rise (GPR) and then the surface potential on the earth due discharging current into

ground grid is known. The touch and step voltages are calculated from surface potential. The duality expression is used to calculate the ground resistance  $R_g$  from the following equation.

$$C = \frac{\sum_{j=1}^n Q_j}{V} \quad (4.5)$$

$n$  is the number of point charges

$$R_g \times C = \rho \times \epsilon$$

where,  $C$  is the capacitance of the grounding grid,  $V$  is the voltage that is defined 1 V,  $Q_j$  is the charge of point charge  $j$  that used for the calculation,  $\rho$  is the soil resistivity and  $\epsilon$  is the soil permittivity.

The CSM is applied to the uniform soil models and it is possible to extend it to other soil models (two-layer soils). The field computation for the two-layer soil system is somewhat complicated due to the fact that the dipoles are realigned in different soils under the influence of the applied voltage. Such realignment of dipoles produces a net surface charge on the dielectric interface. Thus in addition to the electrodes, each dielectric interface needs to be simulated by fictitious point charges. Here, it is important to note that the interface boundary does not correspond to an equipotential surface. Moreover, it must be possible to calculate the electric field on both sides of the interface boundary.





# Chapter 5

## Calculation Results

In this chapter, the results using the Boundary Element Method and the Charge Simulation Method are presented. The results using Boundary Element Method are carried out by using the results from software as mentioned before. On the other hand, the results from a more accurate and practical method (Charge Simulation Method) is presented to calculate the Earth Surface Potential due to discharging impulse current into grounding grid. The results by using this method explain that the method is very good agreement with the empirical formula in IEEE Standard [17], with the Boundary Element Method [29-36] and with the Experimental results using scale model.

### 5.1 Calculation results using BEM

#### 5.1.1 Importance of vertical rods addition to grounding grid

Vertical ground rods are the simplest and commonly used means for earth termination of electrical and lightning protection systems. Vertical ground rods are one of the most important solutions when the upper layer of the soil in which the grid is buried, has higher resistivity than that of the lower layer. The addition of the vertical ground rods to the grounding grid achieve a convenient design for grounding system to improve the performance of it by reducing not only the grid resistance but also the step and touch voltages to values that safe for human.

In this section, the effect of the addition of vertical rods to the grounding grid is described. Fig. (5-1) describes the case of study for the grid with the following characteristics  $10 \times 10 \text{ m}^2$ , the radius of the grid conductor (  $r$  ) is 5 mm, the length of vertical rods (  $L_{vr}$  ) is 2m, its radius of (  $r_{vr}$  ) is 5 mm , the grid depth (  $h$  ) is 0.5 m, and the resistivity of the soil (  $\rho$  ) is  $100 \Omega \cdot \text{m}$ .

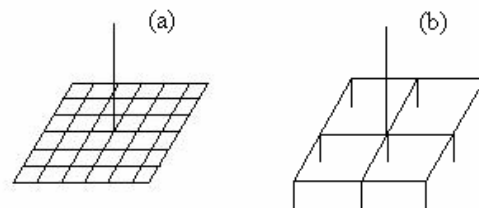


Fig. (5-1) Different grounding grids. (a) 36 meshes. (b) 4 meshes with vertical rods.

The following Table (5-1) explains that an addition of ground rods with 2m lengths to the 4 meshes grounding grid for the case of study gives nearest results when adding the horizontal conductors to the same grid. The difference in the max touch voltage between the two cases is 26.9 V at  $I = 100$  A, and also the max step voltage in the two cases under consideration is the same but the difference in the total length of conductors is 62 m as shown from the table and hence, an increase in the cost of design occurs when adding horizontal rods. Therefore the addition of vertical rods plays an important part to get the good results and decreases the cost of design.

No of meshes	36	4
No. of vertical rods	0	9
Vertical rods length (m)	0	2
Total grid length (m)	140	78
Resistance ( $\Omega$ )	4.3	4.3
GPR (V) at 100 A	426	429
Max touch voltage % GPR	25.0	31.1
Max touch voltage (V)	106.5	133.4
Max step voltage % GPR	16	16

Table (5-1) Comparison between the additional of horizontal rods and vertical rods to the grounding grid.

### 5.1.2 Effect of the vertical rods location on the step and touch voltage

The effect of addition of vertical grounding rods at different locations on Earth Surface Potential (ESP) is investigated. This study describes how a design of grounding grid with vertical rods that achieve the convenient values of ( $R_g$ ,  $V_t$  and  $V_s$ ) with the minimal cost of design can be improved.

The characteristics of the grid are  $50 \times 50$  m<sup>2</sup>, the number of meshes are 4, 16 and 64, the radius of the grid rods ( $r$ ) is 0.005 m, the length of vertical rods ( $L_{vr}$ ) is 2m, the radius of it ( $r_{vr}$ ) is (0.005m), the grid depth ( $h$ ) is 0.5 m, and the resistivity of the soil is 2000  $\Omega$ .m. The following Fig. (5-2) explains the models used for the case study which focus on the effect of the location of vertical rods on the value of Earth Surface Potential and on step and touch voltage.

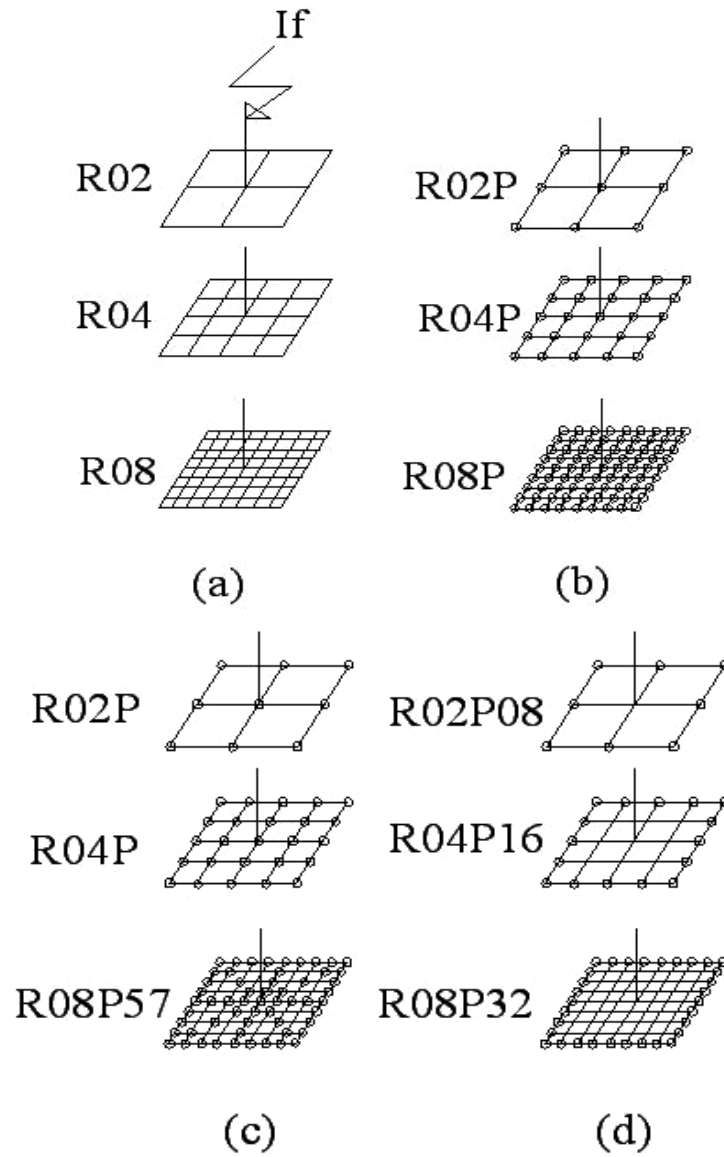


Fig. (5-2) Grounding grids with different meshes and different locations of the vertical rods (a. without vertical rods, b. with vertical rods at all point, c. the vertical rods at the points across the diagonal and center lines, d. the vertical rods at the perimeter of the grid only), the small circles indicate the location of the vertical rods.

Table (5-2) introduces the values of ground grid resistance, step and touch voltages for the different locations of the vertical rods in the grounding grids and fault current ( $I_f$ ) is 1000 A.

Case	$l_t$ (m)	$R_g$ (ohm)	GPR (kV)	$V_{t \max}$ % of GPR	$V_{s \max}$ % of GPR
R02	300	23.1	23.1	41.4	17
R04	500	20.3	20.3	29	16
R08	900	18.6	18.6	20	12
R02P	318	22.7	22.7	40.9	20
R04P	550	19.9	19.9	28	16
R08P	1062	18.1	18.1	17.81	15
R08P57	1014	18.1	18.1	17.92	15
R02P08	316	22.7	22.7	40.92	18
R04P16	532	19.9	19.9	28	16
R08P32	964	18.2	18.2	18.08	15

Table (5-2) GPR, max step voltage, max touch voltage, grounding resistances for different cases.

It is clear from the table that if the number of meshes increases (increase of the horizontal conductors) the grid resistance, step and touch voltages decrease but we should take into account the total length of the conductors used in the grid (the cost of the grounding system), for example the case R08P gives good results but the length of copper used is 1062 m in this case. That means that the cost for this design is much higher than for the case R04P16. R04P16 can be selected as a good compromise between technical and economics aspects.

After studying the effect of the vertical rods and its location which connected to the grounding grids buried in the homogenous soil on the earth surface potential, it is observed that the change of vertical rod locations, a small reduction in the Earth Surface Potential and a considerable reduction in ground potential rise. That means, it is not convenient to use the vertical rods with grounding grid buried in homogenous soil because the economical cost of the grounding grid design should taken into account.

### 5.1.3 Effect of the profile location on step and touch voltages

The effect of profile location (The profile which determines the location of the person above the grounding grid) on some parameters such as the value of step and touch voltages is investigated, and also presents some cases of grid configurations with and without vertical

rods to explain the variations of these parameters with the variations of profile location. Fig. (5-3) explains grounding grids with different profile locations.

The characteristics of the grid are  $20 \times 20 \text{ m}^2$  and also  $10 \times 40 \text{ m}^2$ , the number of meshes are 4, 16 and 36, the radius of the grid rods ( $r$ ) is 0.005 m, the length of vertical rods ( $L_{vr}$ ) is 2m, and its radius ( $r_{vr}$ ) is (0.005m), the grid depth ( $h$ ) is 0.5 m, and the resistivity of the soil ( $\rho$ ) is 100 ohm-m.

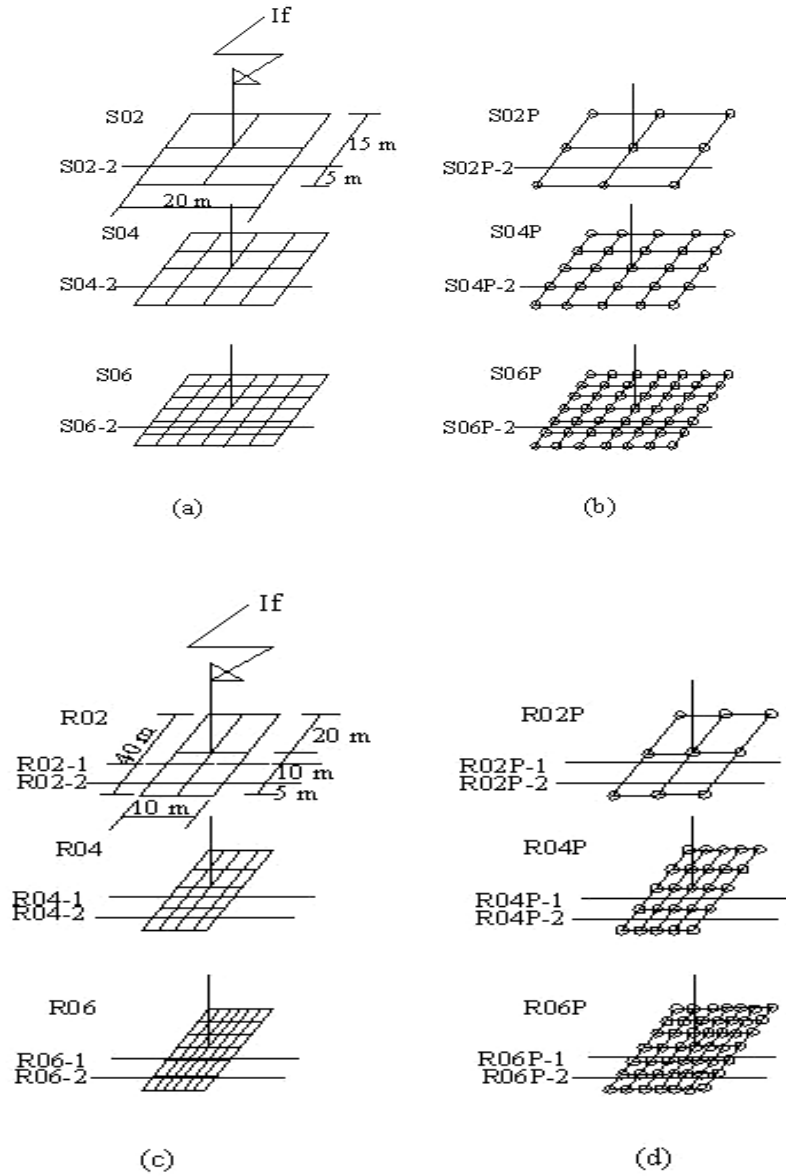


Fig. (5-3) Grounding grids with different profile locations (a. square grids ( $20 \times 20 \text{ m}$ ) without vertical rods, b. square grids ( $20 \times 20 \text{ m}$ ) with vertical rods at all point, c. rectangle grids ( $10 \times 40 \text{ m}$ ) without vertical rods, d. rectangle grids ( $10 \times 40 \text{ m}$ ) with vertical rods at all point).

Table (5-3) shows the values of ground grid resistance, step and touch voltages for the different profile locations of different configurations of grounding grids for fault current ( $I_f$ ) of 100 A.

Case	R (ohm)	GPR (V)	$V_{s,max}/GPR$	$V_{t,max}/GPR$	$I_f$ at GPR=1
R02_1	2.2734	227.34	0.096	0.2566	0.4398
R02_2	2.2734	227.34	0.096	0.2918	0.4398
R02P_1	2.17974	217.97	0.091	0.2567	0.4398
R02P_2	2.17974	217.97	0.100	0.2751	0.4398
R04_1	2.07949	207.94	0.091	0.1622	0.4808
R04_2	2.07949	207.94	0.12	0.17	0.4808
R04P_1	1.96563	196.56	0.073	0.1567	0.5087
R04P_2	1.96563	196.56	0.093	0.168	0.5087
R06_1	2.00472	200.47	0.099	0.1184	0.4988
R06_2	2.00472	200.47	0.114	0.132	0.4988
R06P_1	1.86854	186.85	0.082	0.116	0.5351
R06P_2	1.86854	186.85	0.101	0.1162	0.5351
S02_2	2.62687	262.68	0.111	0.3557	0.3806
S02P_2	2.49163	249.16	0.1	0.336	0.4013
S04_2	2.36307	236.30	0.144	0.1346	0.4231
S04P_2	2.2007	220.07	0.133	0.1143	0.4539
S06_2	2.26078	226.07	0.110	0.151	0.4423
S06P_2	2.07287	207.28	0.096	0.1214	0.4824

Table (5-3) The values of ground grid resistance, step and touch voltages for the different profile locations of different configurations of grounding grids for fault current ( $I_f$ ) of 100 A.

It is clear from Table (5-3) that if the number of meshes increases the grid resistance then the step and touch voltages decrease. The rectangular grid offers good values of the parameters (grid resistance, step and touch voltages) and then represents an improved design for grounding systems. The profile location also plays a great deal for reducing the values of these parameters, the touch voltage decreases when the profile location comes near to the center line of grid.

Table (5-4) shows the validation of the Boundary Element Method for finding the resistance of grounding grid compared the IEEE standard empirical formula [17].

Configuration	Vertical rods	Meshes	Dwight	Laurent	Sverak	Schwarz	BEM
Square 20*20 m <sup>2</sup>	Without	4	2.2150	3.0483	2.9570	2.4230	2.62687
		16	2.2150	2.7150	2.6236	2.1721	2.36307
		36	2.2150	2.5721	2.4808	2.0447	2.26078
	With	4	2.2150	2.9396	2.8483	2.3469	2.49163
		16	2.2150	2.6150	2.5236	2.0846	2.2007
		36	2.2150	2.4796	2.3882	1.9527	2.07287
Rectangle 40*10 m <sup>2</sup>	Without	4	2.2150	2.8817	2.7903	2.0919	2.2734
		16	2.2150	2.6150	2.5236	1.9572	2.07949
		36	2.2150	2.5007	2.4094	1.8836	2.00472
	With	4	2.2150	2.8102	2.7189	2.0599	2.17974
		16	2.2150	2.5483	2.4570	1.9157	1.96563
		36	2.2150	2.4382	2.3469	1.8374	1.86854

Table (5-4) Comparison between the grounding resistance for Boundary Element Method and IEEE standard formulas.

## 5.2 Calculation results using CSM

### 5.2.1 Effect of the number of meshes on the earth surface potential

In this section, the results from using the proposed method (CSM) are presented; some graphs explain the Earth Surface Potential along diagonal profile for the square grid with different number of meshes. The characteristics of the grid are 50x50 m<sup>2</sup>, the radius of the grid rods ( r ) is 8 mm, the grid depth (h) is 0.5 m, the resistivity of the soil (ρ) is 100 Ω.m, and the total ground potential rise (GPR) is defined as 1.

From Fig. (5-4), the number of meshes plays a great part for decreasing the ground grid resistance and also the ground potential rise (GPR) and then decrease the touch and step voltages. When the number of meshes increases the ground surface potential much flatten and



then the step and touch voltages are small and when the number of meshes increases to 144 meshes the touch voltage may be diminished [22].

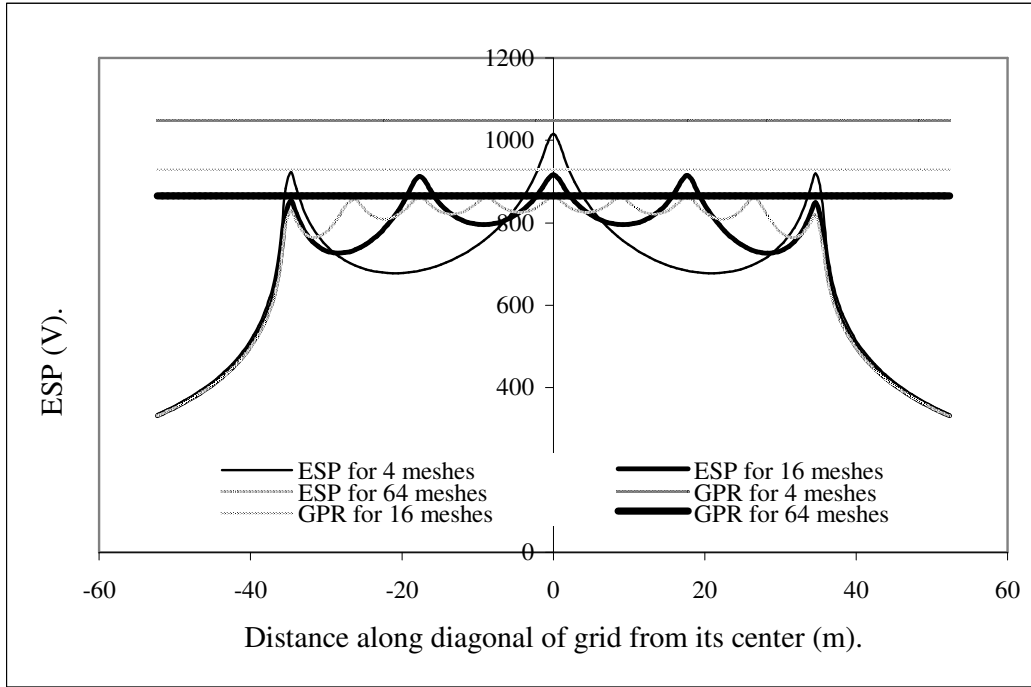


Fig. (5-4) Effect of number of meshes on earth surface potential.

### 5.2.2 Effect of the vertical rods and its length on the earth surface potential

The vertical ground rods penetrate the lower soil layers have many advantages in comparison to a grid alone. Sufficiently long ground rods stabilize the performance of such combined system (grounding grids that connected to vertical rods) making it less dependent on seasonal and weather variations of the soil resistivity. Rods are more efficient in dissipating fault currents because the upper soil layer usually has a higher resistivity than the bottom layers. The current in the ground rods is discharged mainly in the lower portion of the rods. Therefore, the touch and step voltages reduced significantly compared to that of the grid alone. In Fig. (5-5), the vertical rod 3m length is connected to the 16 meshes grid and from the results, small change in the ground potential rise is seen because the homogenous soil is assumed. Also in Fig. (5-6), the vertical rod length has an effect on the earth surface potential.

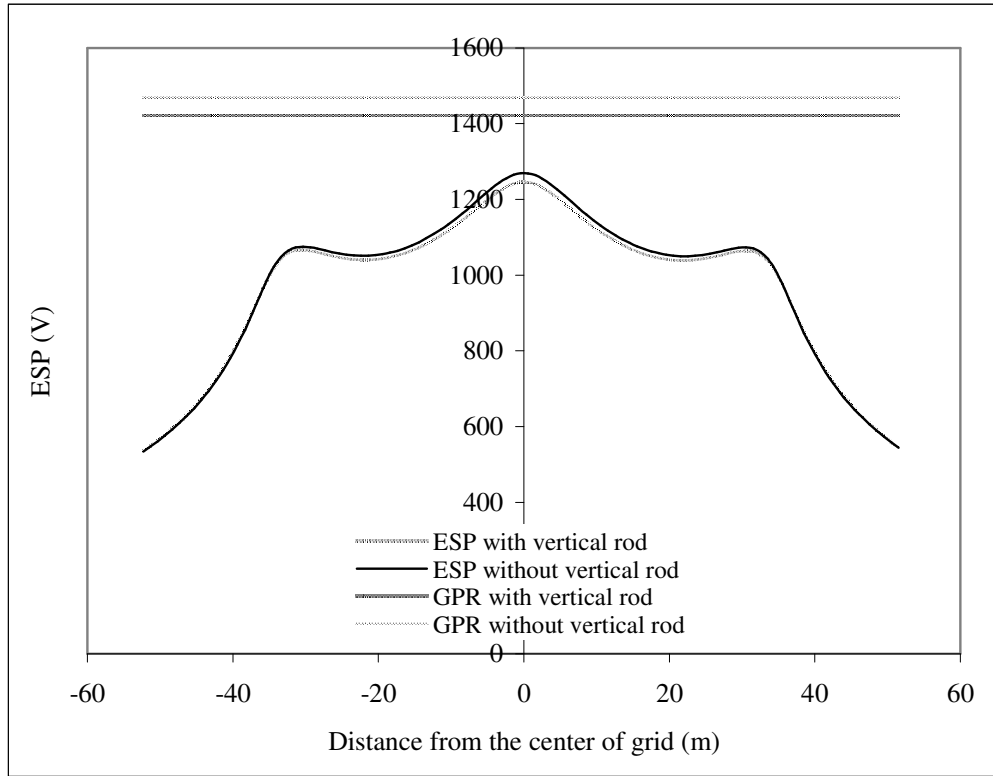


Fig. (5-5) Effect of vertical rods addition to the grids on earth surface potential.

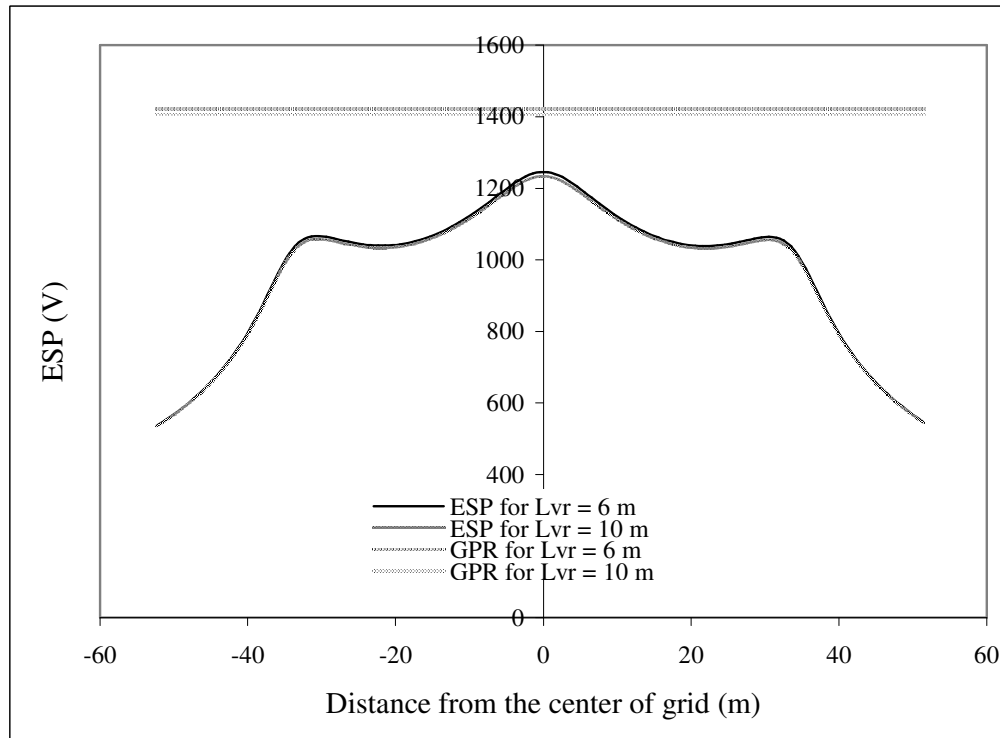


Fig. (5-6) Effect of vertical rods length to the grids on earth surface potential.

### 5.2.3 Effect of grid depth on the earth surface potential

The effect of the grid depth is showed in Fig. (5-7), there, an increase of the grid depth results in the decrease in the grid resistance and also decreases the ground potential rise and earth surface potential. As the result the touch voltage decreases with an increase of the grid depth.

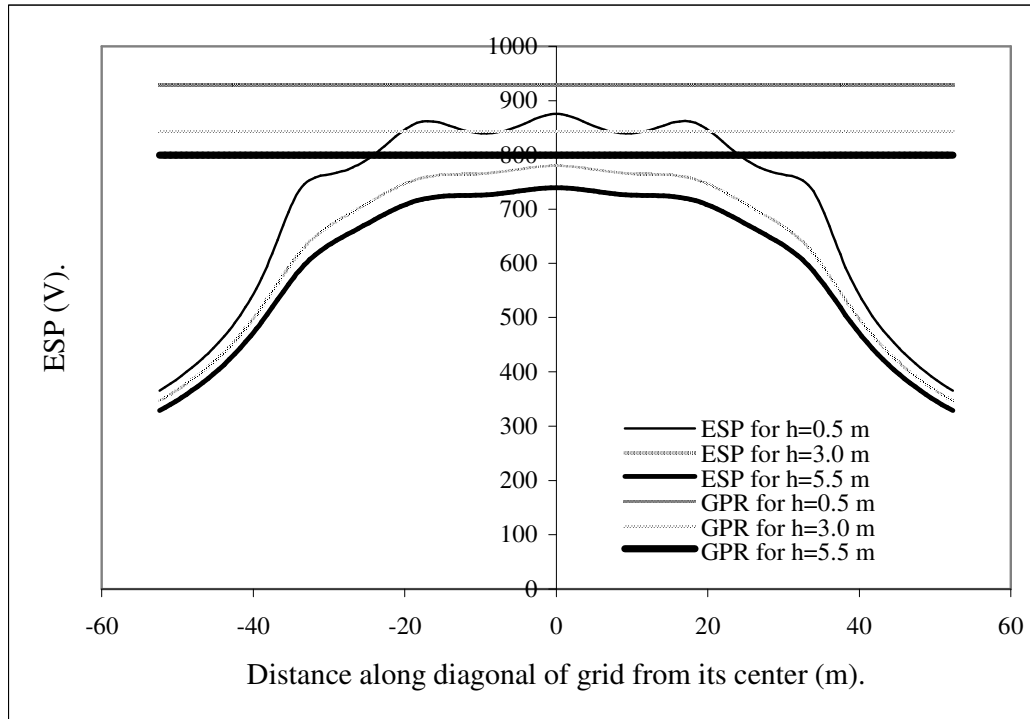


Fig. (5-7) Effect of grid depth on earth surface potential.

### 5.2.4 Effect of number of point charges on the Earth Surface Potential

Fig. (5-8) describes the effect of point charges on Earth Surface Potential and from Fig. (5-8), the small effect is seen when the number of point charges changes, but the increase of the number of point charges result in the time of calculation increases because the increase of the elements of the potential coefficient matrix and also we need a large memory for the CPU to execute this process.

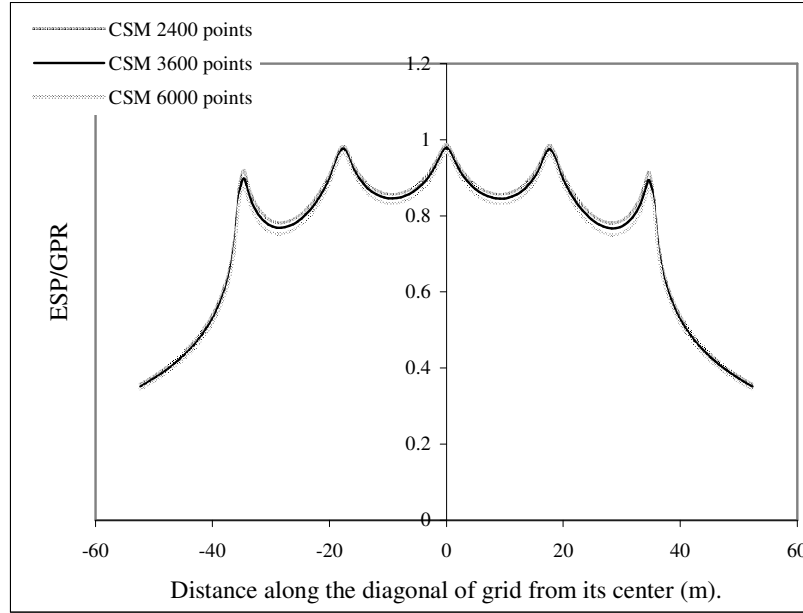


Fig. (5-8) Effect of number of point charges on earth surface potential.

### 5.3 Validation of the Charge Simulation Method

To satisfy the validation of the method, the case of study is taken as the following, the input data about the grid configuration:

Number of meshes (N) = 4, side length of the grid in X direction (X) = 50 m, side length of the grid in Y direction (Y) = 50 m, grid conductor radius = 8 mm, vertical rod length (Z) = 0 (no vertical rod), depth of the grid (h) = 0.5 m, resistivity of the soil ( $\rho$ ) = 100  $\Omega$ .m and the permittivity of the soil is 9.

The following Table (5-5) explains that the result from the proposed method is close to the other formula in [17] and also the values of resistance that calculated by [29-37].

Formula	Resistance ( $\Omega$ )
Dwight[17]	0.8860
Laurent[17]	1.2193
Sverak[17]	1.2086
BEM [29-36]	1.12
Schwarz[17]	1.0415
CSM [37]	1.0479

Table (5-5) Comparison between the grounding resistance for the proposed method and the IEEE standard formulas and also the Boundary Element Method.

Figs. (5-9) and (5-10) explain that the proposed method satisfies an agreement with the other method that used to calculate surface potential for example Boundary Element Method [29-36].

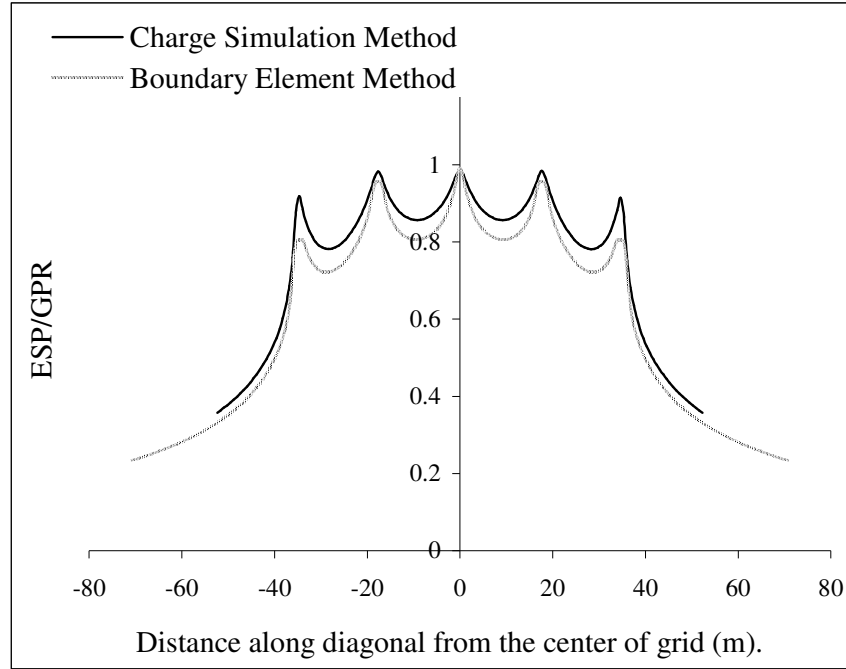


Fig. (5-9) Comparison between proposed method and Boundary Element Method for 16 meshes grid without vertical rods.

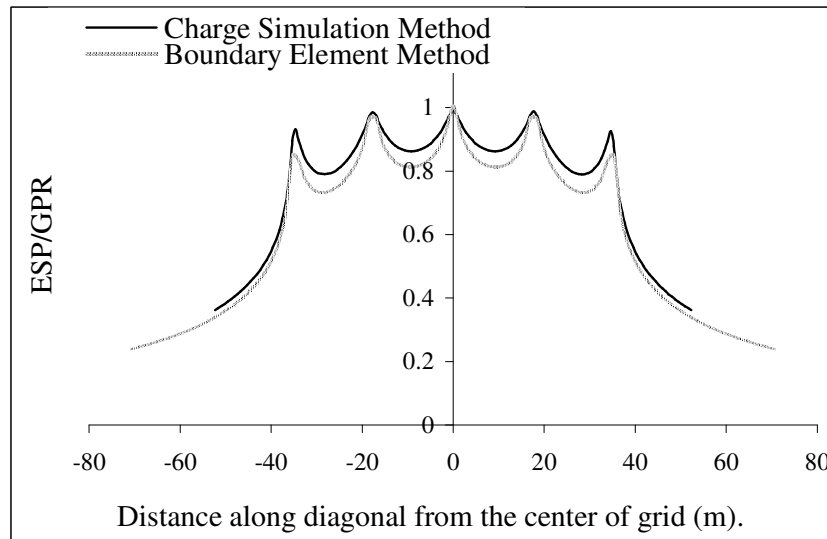


Fig. (5-10) Comparison between proposed method and Boundary Element Method for 16 meshes grid with vertical rods (2m length).

## 5.4 Comparison between the experimental and theoretical calculation by (Charge Simulation Method)

In this section, the comparison between the results from the Charge Simulation Method and the results from the experimental work is investigated. Fig. (5-11) explains the Earth Surface Potential results from the running of the computer program based on the Charge Simulation Method with the reality case which its characteristics are;

The characteristics of the 16 meshes grid are  $50 \times 50 \text{ m}^2$ , the radius of the grid rods (  $r$  ) is 8 mm, the grid depth (  $h$  ) is 2.5 m, the resistivity of the soil (  $\rho$  ) is  $625 \Omega \cdot \text{m}$ .

Table (5-6) shows the Earth Surface Potential (ESP) at the points described in the figure (3.8).

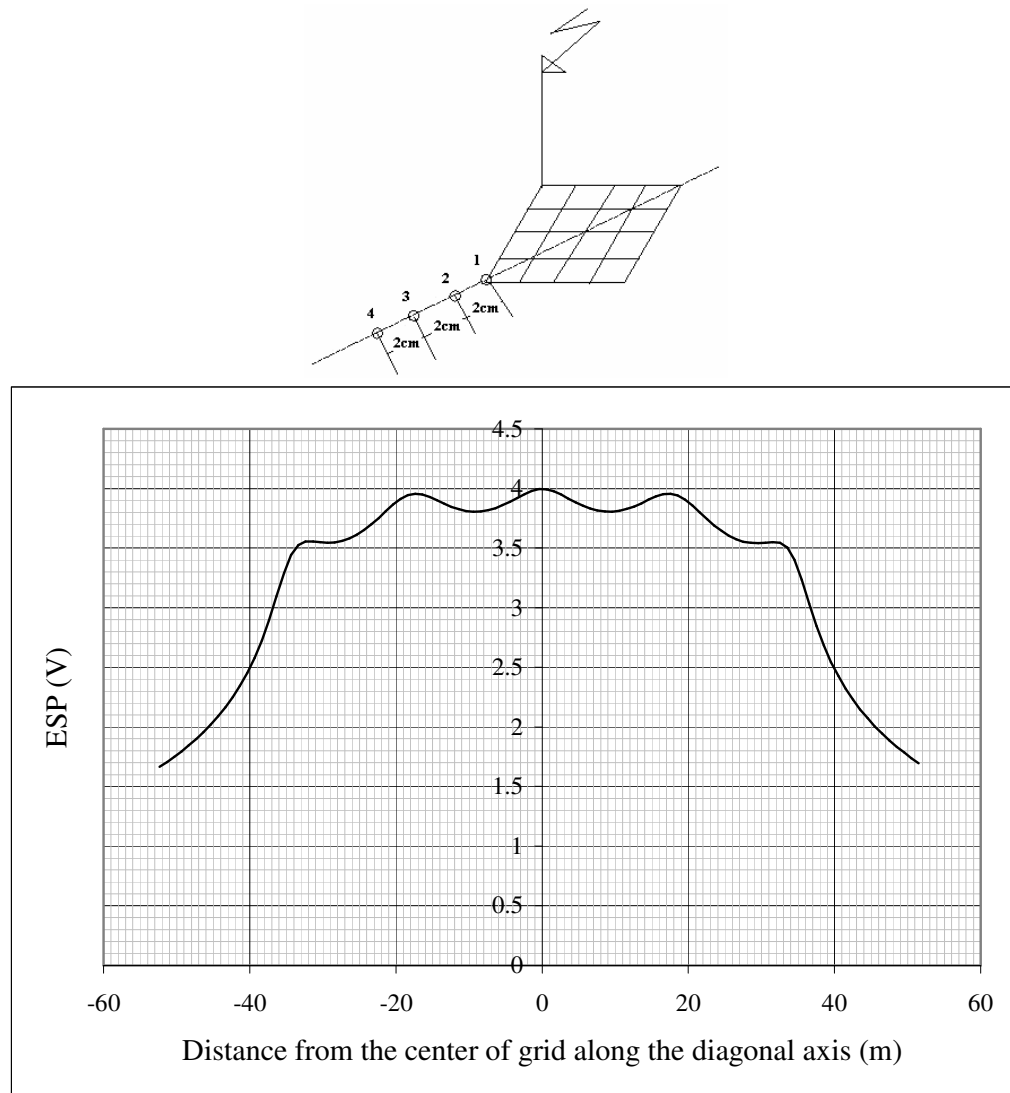


Fig. (5-11) Earth Surface Potential profile for real model.

	Distance	ESP/GPR	ESP (V)
Point 1	33.5	0.844	3.50
Point 2	35.5	0.779	3.23
Point 3	37.5	0.686	2.85
Point 4	39.5	0.613	2.54

Table (5-6) Voltage differences at specified points as in Fig. (3-8).

From Table (5-7), the voltage difference is calculated between each of two points and compare the results with the scale model results that shown in Fig. (3-13a, 13b, 14a, 14b, 15a, 15b);

Voltage difference from the Figs. (3-13a, 13b, 14a, 14b, 15a, 15b)					
$V_{12}$ (mV)	370	$V_{23}$ (mV)	300	$V_{34}$ (mV)	290
$V_{21}$ (mV)	250	$V_{32}$ (mV)	300	$V_{43}$ (mV)	310
$V_{ave}$ (mV)	310	$V_{ave}$ (mV)	300	$V_{ave}$ (mV)	300
Voltage difference (calculated) from Table (5-6)					
$V_{12}$ (mV)	270	$V_{23}$ (mV)	380	$V_{34}$ (mV)	310
Error $\% = (V_{ave} - V_{cal}) / V_{ave}$	12.9	Error %	-26.67	Error %	-3.3

Table (5-7) Comparison between the results from the proposed method and the scale model.

It is seen from Table (5-7) that the max absolute error is 26.67 % and the minimum one is 3.2%. Then the results from the proposed method to calculate the Earth Surface Potential due to discharging impulse current into grounding grid is acceptable and reliable for two reasons:

The first one, there are no oscillations accompanied with the waveforms of the measured voltage and then the transient behaviour can be ignored and the static behaviour is enough for calculation by the proposed method.

The second reason, the average of the absolute error from the Table (5-7) is 14.3 % and this may be acceptable for the calculation by the proposed method.





# Chapter 6

## Optimization of Grounding Grids Design Based on Evolutionary Strategy

An Evolutionary Strategy is a process of continuous reproduction, trail and selection. Each new generation is an improvement on the one that went before. This results in systems that become increasingly more efficient and more organized.

Evolutionary Strategies (ESs), were first developed by Fogel [58], and Schwefel [59], in the early sixties. They stress the behavioral (as opposed to genetic) connection between the current generation and the next generation. ESs have also been shown to converge linearly (in the number of generations) [60] an order of convergence, which according to Voigt [61], is the best possible performance for evolutionary algorithms (which include ESs). In addition, [60] shows that given unlimited time, elitist evolutionary algorithms, would produce a globally optimal solution with probability one, and that that holds, under rather general conditions. This again is untrue for canonical GAs [62]. Hence, it was decided to use an Evolutionary Strategy to optimize our system.

In the field of grounding systems design, the optimization means that how these grounding systems not only safeguard those people that working or walking in the surroundings of the grounded installations, but also minimize the cost of design.

The use of an Evolutionary Computation (EC) technique for the optimization of a grid design algorithm allows for the attainment of optimal fitness (i.e. the best choice of parameter values) through an automated process.

The process of optimization, if done manually, can be extremely time-consuming, requiring a lot of intelligent guessing without, at the same time, offering any guarantee of suitable results.

Additionally, every time there may be a change of domain, the process will need reconfiguration to suit its new environment, which requires expert knowledge. This process of reconfiguration might take the same length of time as the initial tuning of parameter values.

In this chapter, a new application is proposed for getting the optimum design of grounding systems. The basic design quantities of the grounding grids are the ground resistance ( $R_g$ ), the ground potential rise (GPR), touch and step voltages.

These mentioned quantities depend on the grid parameters, which are its side lengths, radius of grid conductors and length of vertical rods. The dependence of the design quantities of the geometric parameters is given by field computation based on equivalent charges using Charge Simulation Method (CSM).

## 6.1 Evolutionary Algorithm (Optimizer)

A Genetic or Evolutionary Algorithm applies the principles of evolution found in nature to the problem of finding an optimal solution to a Solver problem. In a "Genetic Algorithm" the problem is encoded in a series of bit strings that are manipulated by the algorithm; in an "Evolutionary Algorithm" the decision variables and problem functions are used directly.

Figs. (6-1) and (6-2) explain the Evolutionary Algorithm that used to introduce the optimum design of grounding grids and its flow chart that explain how this algorithm works.

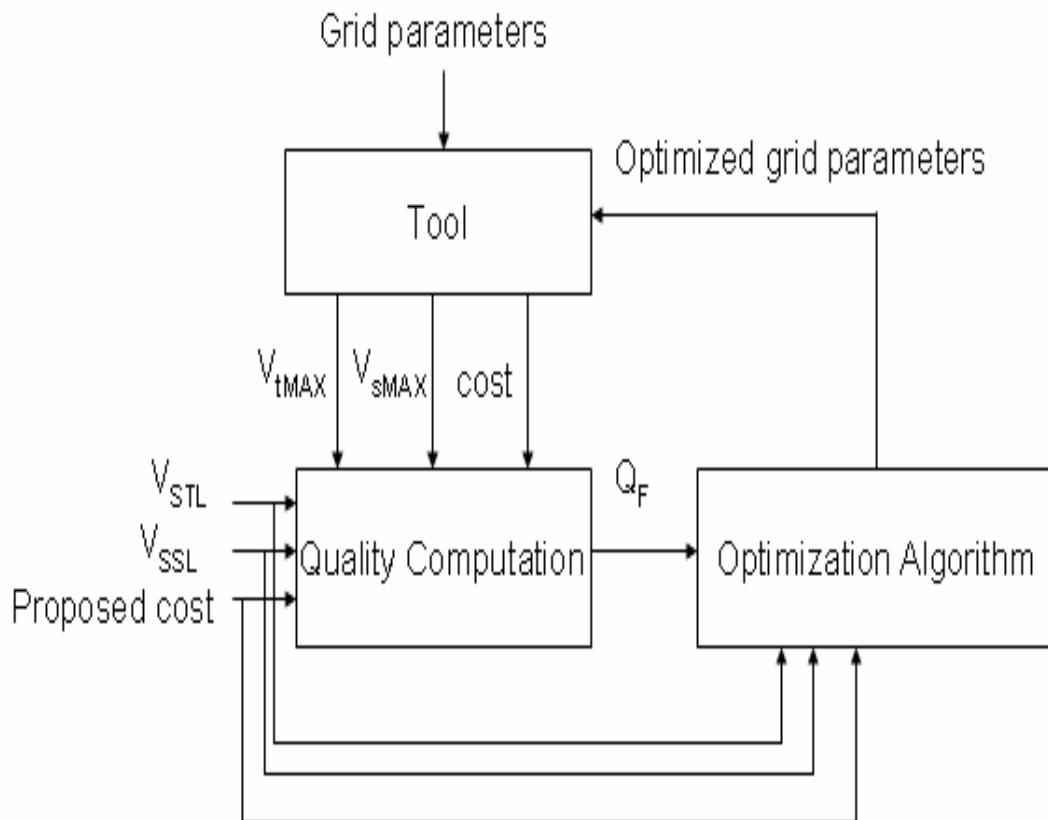


Fig. (6-1) Evolutionary Strategy model for optimization the design of grounding grids.

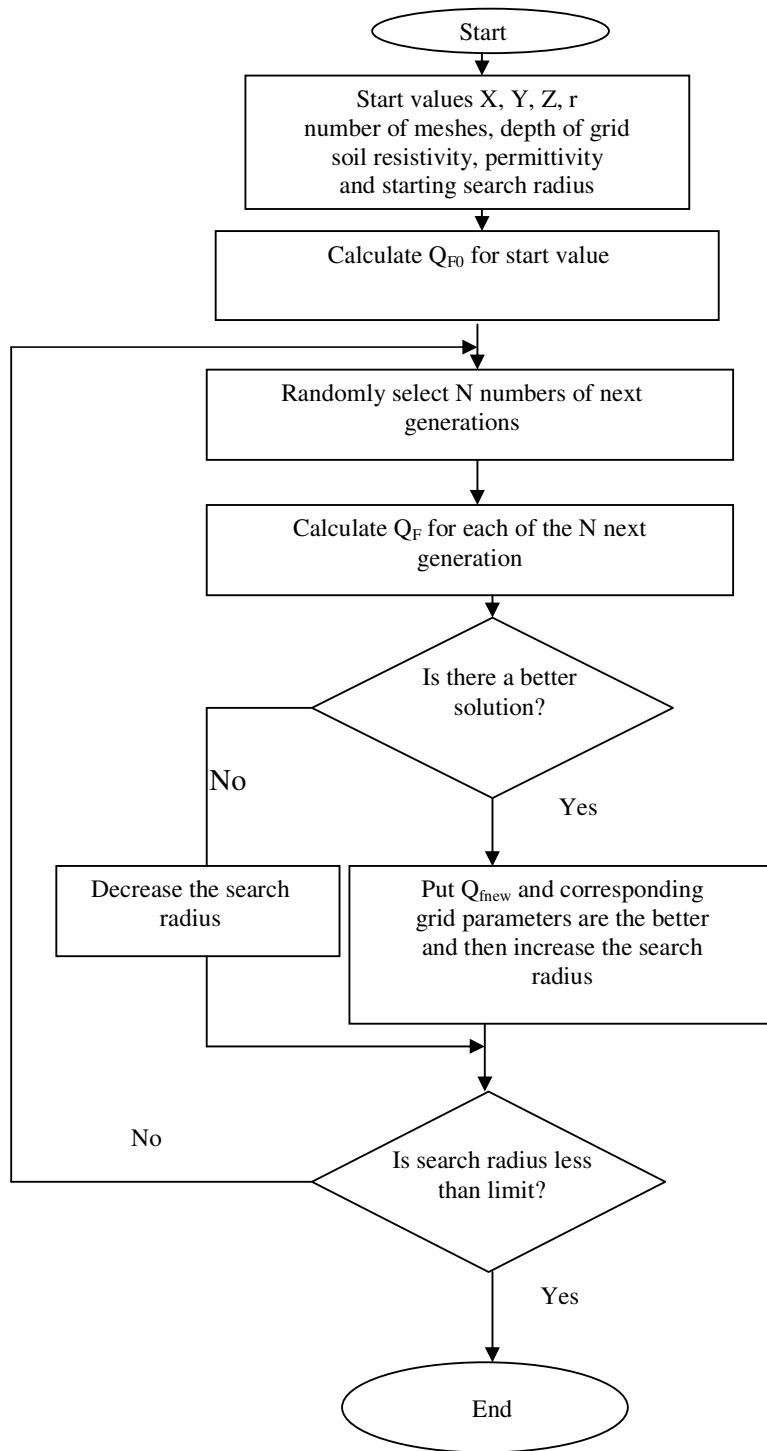


Fig. (6-2) Flow chart of the program based on Evolutionary Strategy to optimize the grounding grid design.

The tool box in Fig. (6-1) involves the CSM technique that used to calculate Earth Surface Potential and also the equations that calculate the touch voltage, step voltage and the total cost of the design and then compare these results with the safe limit value for touch voltage, step voltage and the cost at the same case to get the quality factor.

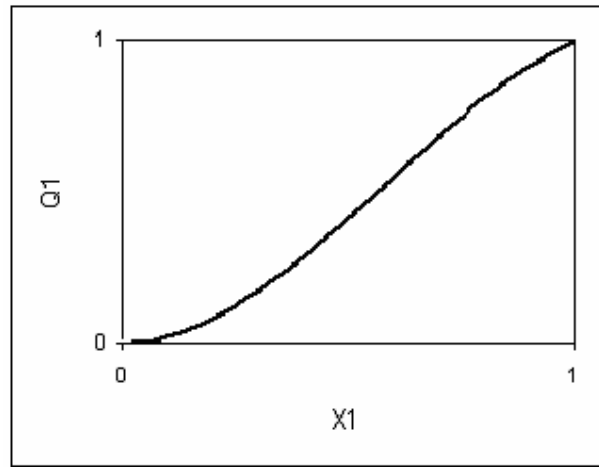
The flow chart in Fig. (6-2) explains how the algorithm is working, in the first; the calculation of the Earth Surface Potential, touch and step voltage and the cost of design is carried out. Therefore the initial quality factor which is based on the pervious quantities is calculated according to the objective function as described in Fig. (6-3). The algorithm starts to choose the random values for the grid dimensions with 10 next generations to get the best quality factor from new generations. Then, the algorithm compare between the initial values of the quality factor with the best value from the next generation to specify the grid dimensions that satisfy optimization case. The algorithm repeats this process until the search radius of the variation parameters are less than the limit condition which is 0.1 of the initial variation parameters.

The following equation (6.1) explains that the quality factor depend on the grid parameters [63].

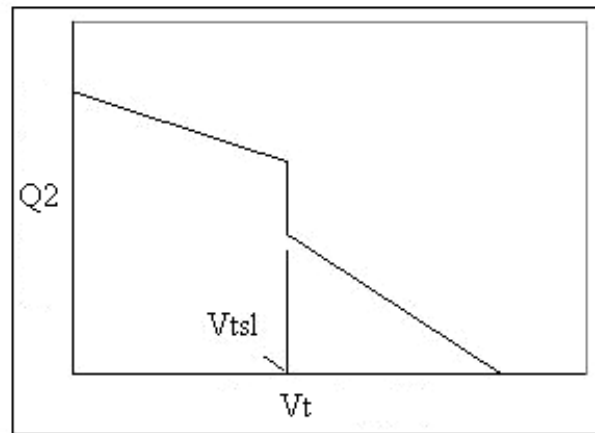
$$\begin{aligned}
 Q_F &= f_1(Q_i), \quad i = 1, 2, 3 \\
 Q_1 &= \begin{cases} f_2(\text{proposed cost}, \text{cost}) & \text{for proposed cost} > \text{cost} \\ 0 & \text{for proposed cost} \leq \text{cost} \end{cases} \\
 Q_2 &= f_3(V_{tsl}, V_t) \\
 Q_3 &= f_4(V_{ssl}, V_s) \\
 \text{Cost}, V_t, V_s &= f_5(X, Y, Z)
 \end{aligned} \tag{6.1}$$

where,  $Q_F$  is the total quality factor,  $V_t$ ,  $V_s$  are the calculated touch and step voltages,  $V_{tsl}$ ,  $V_{ssl}$  are the safe limit of touch and step voltages at the case study,  $X$  is the side length of the grid in x direction,  $Y$  is the side length of the grid in y direction,  $Z$  is the length of the vertical rod if available and  $r$  is the grid conductor radius.

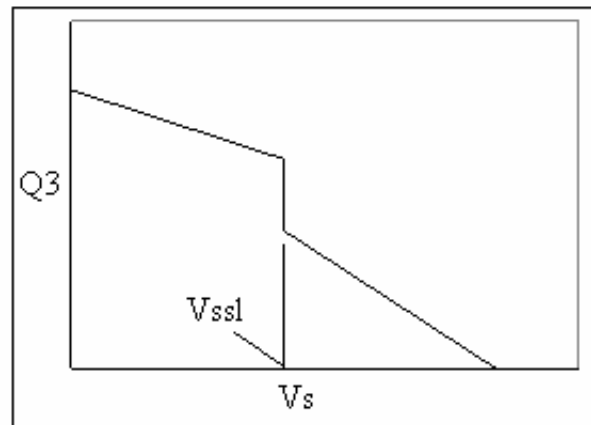
Fig. (6-3a, b, c) illustrates the objective function that involved in the algorithm. In Fig. (6-3a)  $x_I$  is ((proposed cost-cost)/cost).



(a)



(b)



(c)

Fig. (6-3a, b, c) The relationships between the quality factors and (cost,  $V_t$ ,  $V_s$ ).

## 6.2 Numerical Example

In this section, the numerical example is produced to explain the input and output data for the algorithm and how this algorithm help us to give the optimum design of grounding grid that satisfy the safe condition for people that working or walking in the surroundings of the grounded installations.

Starting values of the grid configuration:

Number of meshes (N) = 4, side length of the grid in x direction (X) = 70 m, side length of the grid in y direction (Y) = 70 m, grid conductor radius = 10 mm, vertical rod length (Z) = 0 (no vertical rod), depth of the grid (h) = 0.5 m, resistivity of the soil ( $\rho$ ) = 100  $\Omega$ .m, the threshold value of safe touch and step voltages are computed from equation (1.4b) and (1.7b) taking into account that the back up fault clearing time is 1 s with the soil resistivity 100  $\Omega$ .m uniform soil. The safe limit of the touch and step are  $V_{tsl} = 180$  V and  $V_{ssl} = 251$  V, the proposed cost is assumed 1000 Euro, the search radius is 0.25 of the variation parameters, the number of next generations is 10.

Table (6-1) shows the values of touch, step voltages and the cost at the starting of the design and after using the optimization algorithm.

	$V_t$ (V)	$V_s$ (V)	Cost (Euro)	Number of meshes	Dimension
Starting design	242.7	123.4	332	4	70*70 m <sup>2</sup>
Optimized design	25.8	47	494	4	235.65*75.894 m <sup>2</sup>
Starting design	105.6	67.62	451.2	16	80*80 m <sup>2</sup>
Optimized design	92.27	76.7	498	16	95.4*94.6 m <sup>2</sup>

Table (6-1) Optimization design results.

The cost of the optimized design is higher than at starting design but is still lower than the proposed cost. The very important issue for the optimization that the touch and step voltage must be lower than the safe limit value. From the table the optimization algorithm able to decrease the touch and step and keep the cost lower than the proposed cost. As seen in the second case for 16 meshes grid the touch and step voltages at the starting value (80\*80 m<sup>2</sup>) are lower than the safe limit values but the program is able to get another grid design with higher quality factor which means the reduction in touch voltage value.

As in [22] the radius of the conductor of the grid has very small effect on the Earth Surface Potential as well as on the touch and step voltage, therefore the radius of the conductor is constant at the processing of the optimization.





# Chapter 7

## Conclusions

The thesis aims to calculate the Earth Surface Potential due to discharging current into grounding grid by using a scale model with electrolytic tank. If all dimensions of the grid and the time of the current waveshape are reduced by the same factor the current waveshape and the equipotential surface distribution unaltered but and then the results from this model can be used as guidelines for safe design of grounding systems. The waveshaps of the measured voltage difference under transient behavior have not any oscillations and therefore, the static model can be used to calculate the earth surface potential.

The pervious observation from the using scale model inspires us to use an old method but it is more accurate and practical method to determine the Earth Surface Potential above the grounding grid, which is the Charge Simulation Method (CSM). Some other calculations are made by using software package (TOTBEM) based on the Boundary Element Method (BEM) to compare between the two methods. The CSM gives a good agreement with the (BEM).The validation of the two methods is satisfying by a comparison between their results and the results based on the empirical formulas in IEEE standard for the grounding grid resistance calculation. The validation of the CSM is satisfied also from the comparison between the results from it and the experimental work which explains that the average error between them is 14.3 % and this is in the range of acceptable.

The results explain that the vertical rods play an important role for reducing the grid resistance, the step and touch voltages. The number of meshes is an effective parameter for reducing the pervious values but it needs more copper then increases the cost. The study explains a small effect in the Earth Surface Potential when changing the vertical rods locations at the same number of meshes hence the economical cost plays a great part for choosing the suitable design for the square grids, some cases give suitable results for the grid resistance, step and touch voltages and in the same time it presents an economical cost.

The thesis demonstrates that another important parameter that effects in the pervious values is the profile location. The man location in case of fault determines the value of step and touch voltage that exposed. The results shows that the dangerous point is at the side of the grid and comes in the corner mesh in the grid.

In the field of grounding systems design, the optimization of the grounding system design means that how these grounding systems safeguard those people that working or walking in the surroundings of the grounded installations from dangerous electrical shocks, as

well as minimizing the cost of design to satisfy optimization. An optimization of the grounding grid design using evolutionary strategy is proposed, which based on a field computation tool (CSM), as a new application that helps not only in designing of grounding systems but also in achieving a suitable economical design.



## References

- [1] R. Verma and D. Mukhedkar, "Fundamental Considerations and Impulse Impedance of Ground Grids", IEEE Transaction on Power Apparatus and Systems, Vol. Pas-100, March 1981, pp. 2053-2059.
- [2] F. Menter and L. Gercevic, "EMTP-Based Model of Grounding System Analysis" IEEE Transactions on Power Delivery, Vol. 9, Oct. 1994, pp. 1838-1849.
- [3] B. Thapar, V. Gerez, A. Balakrishnan, D. A. Blank, "Evaluation of Grounding Resistance of a Grounding Grid of any Shape", IEEE Transactions on Power Delivery, Vol. 6, No. 2, April. 1991, pp. 640-647.
- [4] A. P. S. Meliopoulos, G. Cokkinides, H. Abdallah, S. Duong, S. Patel, "A PC Based Ground Impedance Measurement Instrument", IEEE Transactions on Power Delivery, Vol. 8, No. 3, July 1993, pp. 1095-1106.
- [5] Y. Liu, N. Theethayi, R. Thottappillil, "An Engineering Model for Transient Analysis of Grounding System under Lightning Strikes: Nonuniform Transmission Line Approach", IEEE Transactions on Power Delivery, Vol. 20, No. 2, April 2005, pp. 722-730.
- [6] Y. Liu, M. Zitnik, R. Thottappillil, "An Improved Transmission Line Model of Grounding System", IEEE Transactions on Power Delivery, Vol. 43, No. 3, August 2001, pp. 348-355.
- [7] S. Karaki, T. Yamazaki, K. Nojima, T. Yokota, H. Murase, H. Takahashi, S. Kojima, "Transient Impedance of GIS Grounding Grid", IEEE Transactions on Power Delivery, Vol. 10, No. 2, April 1995, pp. 723-731.
- [8] A. Geri, "Behaviour of Grounding Systems Excited by High Impulse Currents: the Model and its Validation", IEEE Transactions on Power Delivery, Vol. 10, No. 2, April 1995, pp. 723-731.
- [9] M. Andre, F. Mattos, "Grounding Grids Transient Simulation", IEEE Transactions on Power Delivery, Vol. 20, No. 2, April 2005, pp. 1370-1378.
- [10] R. Zeng, J. He, Z. Guan, "Novel Measurement System for Grounding Impedance of Substation", IEEE Transactions on Power Delivery, Vol. 21, No. 2, April 2006, pp. 719-725.
- [11] Y. L. Chow, M. M. A. Salama, "A Simplified Method for Calculating the Substation Grounding Grid Resistance", IEEE Transactions on Power Delivery, Vol. 9, No. 2, April 1994, pp. 736-742.
- [12] B. R. Gupta, V. K. Singh, "Impulse Impedance of Grounding Grids", IEEE Transactions on Power Delivery, Vol. 7, No. 1, January 1992, pp. 214-218.

## References

- [13] S. Sekioka, M. I. Lorentzou, M. P. Philippakou, J. M. Prousalidis, "Current –Dependent Grounding Resistance Model Based on Energy Balance of Soil Ionization", IEEE Transactions on Power Delivery, Vol. 21, No. 1, January 2006, pp. 194-201.
- [14] M. Tsumura, Y. Babo, N. Nagaoka, A. Ametani, "FDTD Simulation of a Horizontal Grounding Electrode and Modelling of its Equivalent Circuit", IEEE Transactions on Power Delivery, Vol. 48, No. 4, November 2006, pp. 817-825.
- [15] Z. Stojkovic, J. M. Nahman, D. Salamon, B. Bukorovic, "Sensitivity Analysis of Experimentally Determined Grounding Grid Impulse Characteristics", ", IEEE Transactions on Power Delivery, Vol. 13, No. 4, October 1998, pp. 1136-1142.
- [16] C. Mazzetti, G. M. Veca, "Impulse Behaviour of Ground Electrodes", IEEE Transaction on Power Apparatus and Systems, Vol. Pas-102, No. 9, September 1983, pp. 3148-3156.
- [17] IEEE Guide for safety in AC substation grounding, IEEE Std.80-2000.
- [18] S. J. Schwarz, "Analytical Expressions for Resistance of Grounding Systems," AIEE Transactions, vol. 73, part III-B, 1954, pp. 1011-1016.
- [19] E. D. Sunde, Earth Conduction Effects in Transmission Systems, D. Van Nostrand Company Inc., New York 194, 1968.
- [20] G. F. Tagg, Earth Resistances, Pittman Publishing Corporation, London, 1964.
- [21] J. G. Sverak, "Simplified Analysis of Electrical Gradient above a Ground Grid-I", IEEE Transactions on Power Apparatus and Systems, Vol. Pas-103, No. 1, January 1984, pp. 7-25.
- [22] F. Dawalibi, D. Mukhedkar, "Behaviour of Grounding Systems in Multilayer soils: A Parametric Analysis", IEEE Transactions on Power Delivery, Vol. 9, No. 1, January. 1994, pp. 334-342.
- [23] J. Nahman, and S. S Kuletich, "Irregularity Correction Factors for Mesh and Step Voltages of Grounding Grids", IEEE Transactions on Power Apparatus and Systems, Vol. Pas-99, No. 1, Jan/Feb: 1980, pp. 174-179.
- [24] W. Koch, "Erdungsmassnahmen für Höchstspannungsanlagen mit Geerdetem Sternpunkt", Elektrotechnische Zeitschrift, Vol. 71, February 1950, pp. 89-91.
- [25] B. Thapar, V. Gerez, A. Balakrishnan and D. A. Blank, "Simplified Equations for Mesh and Step Voltages in an AC Substation," IEEE Trans. on Power Delivery, vol. 6, No. 2, April 1991, pp 601-607.
- [26] J. M. Nahman, V. B. Djordjevic, "Maximum Step Voltages of Combined Grid-Multiple Rods Ground Electrodes," IEEE Trans. Power Delivery, vol. 13, no. 3, Juli 1998, pp. 757-761.

## References

- [27] J. A. Güemes and F. E. Hernando, "Cálculo de Redes de Tierra Utilizando el Método de Elementos Finitos. Comparación de Resultados," in *Proc.IEEE Andean Región Int. Conf.*, vol. 2, 1997, pp. 902–906.
- [28] J. A. Güemes and F. E. Hernando, "Method for Calculating the Ground Resistance of Grounding Grids Using FEM", *IEEE Trans. Power Delivery*, vol. 19, No. 2, April 2004, pp. 595-600.
- [29] Navarrina F., Colominas I., Casteleiro M., Analytical Integration Techniques for Earthing Grid Computation by BEM, *Num. Met. in Eng. And Appl. Sci.*, 1197-1206, CIMNE, Barcelona, 1992.
- [30] M. Casteleiro, L.A. Hernhdez, I. Colominas and F. Navarrina, "Memory and User Guide of System TOTBEM for CAD of Grounding Grids in Electrical Installations", (in Spanish), Civil Engineering School, Universidad de La Coruña, 1994.
- [31] I. Colominas, F. Navarrina, M. Casteleiro, "Numerical Simulation of Transferred Potentials in Earthing Grids Considering Layered Soil Models", *IEEE Transactions on Power Delivery*, vol. 22, No. 3, 2007, pp.1514-1522.
- [32] I. Colominas, F. Navarrina, and M. Casteleiro, "Analysis of Transferred Earth Potentials in Grounding Systems: A BEM Numerical Approach," *IEEE Trans. Power Delivery*, vol. 20, no. 1, Jan. 2005, pp. 339-345.
- [33] I. Colominas, F. Navarrina, and M. Casteleiro, "A Boundary Element Numerical Approach for Earthing Grid Computation", *Computer Methods in Applied Mechanics and Engineering*, vol. 174, 1990, pp 73-90.
- [34] I. Colominas, F. Navarrina, and M. Casteleiro, "A Numerical Formulation for Grounding Analysis in Stratified Soils", *IEEE Trans. on Power Delivery*, vol. 17, April 2002, pp 587-595.
- [35] F. Navarrina, I. Colominas, "Why Do Computer Methods for Grounding Analysis Produce Anomalous Results?" *IEEE Trans. on Power Delivery*, vol. 18, No. 4, October 2003, pp 1192-1201.
- [36] I. Colominas, "A CAD System for Grounding Grids in Electrical Installations: A Numerical Based on the Boundary Element Integral Method," Ph.D. Dissertation (in Spain), Universidad de A Coruna, Spain, 1995.
- [37] S. Ghoneim, H. Hirsch, A. Elmorshedy, R. Amer, "Charge Simulation Method for Finding Step and Touch Voltage", 15<sup>th</sup> ISH2007, Slovenia, August 2007.

## References

- [38] E. Bendito, A. Carmona, A. M. Encinas and M. J. Jimenez “The Extremal Charges Method in Grounding Grid Design,” IEEE Transaction on Power Delivery, vol. 19, No. 1, January 2004, pp 118-123.
- [39] A. Elmorshedy, A. G. Zeitoun, and M. M. Ghourab, “Modeling of Substation Grounding Grids,” IEE Proceedings, Vol. 133, Pr. C, No. 5, July 1986.
- [40] B. Thapar, and K. K. Pura, “Mesh Potentials in High Voltage Grounding Grids” IEEE Transactions on Power Apparatus and Systems, Vol. Pas-86, 1967, pp. 249-254.
- [41] C. S. Choi, H. K. Kim, H. J. Gil, W. K. Han, and K. Y. Lee, “The Potential Gradient of Ground Surface According to Shapes of Mesh Grid Grounding Electrode Using Reduced Scale Model,” IEEE Trans. On Power and Energy, Vol. 125, no. 12, 2005, pp. 1170.
- [42] I. F. Gonos, “Experimental Study of Transient Behavior of Grounding Grids Using Scale Model”, Measurement science and Technology. 17 (2006), pp. 2022-2026.
- [43] I. F. Gonos, F. V. Topalis, I. A. Atathopoulos "Modeling of a Grounding Grid Using an Electrolytic Tank", 12<sup>th</sup> ISH Symposium, India, 20-24 August, 2001.
- [44] W. Koch, "Grounding Methods for High-Voltage Stations with Grounded Neutrals," translated from Elektrotechnische Zeitschrift, Vol. 71, No. 4, February 1950, pp. 89-91.
- [45] H.R. Armstrong, "Grounding Electrode Characteristics from Model Tests," AIEE Transactions on Power Apparatus and Systems, Vol. 72, Pt. III, December 1953, pp. 1301-1306.
- [46] R.P. Keil, "Model Test to Investigate Fence Grounding in a Substation," Master's Thesis, University of Dayton, Dayton, Ohio, April 1973.
- [47] S. Mukhedkar, Y. Gervais and J. DeJean, "Modeling of a Grounding Electrode," IEEE Transactions on Power Apparatus and Systems, Vol. PAS-92, No.1, January/February 1973, pp. 295-297.
- [48] R. Caldecott, D. G. Kasten, “Scale Model Studies of Station Grounding Grids,” IEEE Trans. Power Apparatus and Systems, Vol. PAS-102, No. 3, 1983, pp. 558-566.
- [49] B. Thapar, S. L. Goyal, “Scale Model Studies of Grounding Grids in Non-Uniform Soils,” IEEE Transactions on Power Delivery, Vol. PWRD-2, No. 4, 1987, pp. 1060-1066.
- [50] S. Ghoneim, H. Hirsch, A. Elmorshedy, R. Amer, "Measurement of Earth Surface Potential Using Scale Model", UPEC2007, Brighton University, England, September 2007.
- [51] L.I. Sedov, Similarity and Dimensional Methods in Mechanics, Science Press, Beijing (1982) (in Chinese).

## References

- [52] J. G. Sverak, "Progress in Step and Touch Voltage Equations of ANSI/IEEE Std. 80," IEEE Trans. Power Del., vol. 13, No. 3, Jul. 1999, pp. 762–767.
- [53] D. L. Garrett and J. G. Pruitt, "Problems Encountered with the APM of Analyzing Substation Grounding Systems," IEEE Trans. Power App. Syst., vol. PAS-104, Dec. 1985, pp. 3586–3596.
- [54] S. Ghoneim, H. Hirsch, A. Elmorshedy, R. Amer, "Surface Potential Calculation for Grounding Grids", IEEE International Power and Energy Conference, PEcon2006, Putra Jaya, Malaysia, Nov. 2006, pp. 501 – 505.
- [55] S. Ghoneim, H. Hirsch, A. Elmorshedy, R. Amer, "Improved Design of Square Grounding Grids", International Conference Power System Technology, POWERCON2006, Chongqing, China, Oct. 2006, pp. 1 – 4.
- [56] N. H. Malik, "A Review of Charge Simulation Method and its Application," IEEE Transaction on Electrical Insulation, vol. 24, No. 1, February 1989, pp 3-20.
- [57] "NUMERICAL RECIPES in C", BOOKS on line, pp. 43-50.
- [58] Fogel, L.J. "Autonomous Automata", in Industrial Research. Vol.4, 1962, pp.14-19.
- [59] Schwefel, H.-P.: "Kybernetische Evolution als Strategie der Experimentellen Forschung in der Strmungstechnik", Diploma thesis, Technical University of Berlin, 1965.
- [60] Back, T., Rudolph, G., and Schwefel, H.- P.: "Evolution Programming and Evolution Strategies: Similarities and Differences", in Fogel, D.B., and Atmar, W. (ed.), Proceedings of the Second Annual Conference on Evolutionary Programming, Evolutionary Programming Society, San Diego, CA, 1993, pp.11-22.
- [61] Voigt, H.-M., Muhlenbein, H., and Cvetkovic, D. "Fuzzy Recombination for the Breeder Genetic Algorithm", in Eshelman, (ed.), Genetic algorithms: Proceedings of the 6<sup>th</sup> International Conference, pp. 104-111, Morgan Kaufmann Publishers, San Francisco, 1995.
- [62] Rudolph, G.: "Convergence Analysis of Canonical Genetic Algorithms", in IEEE Transactions on Neural Networks, Special Issue on Evolutionary Computation, 5(1):96-101, 1994.
- [63] S. Ghoneim, H. Hirsch, A. Elmorshedy, R. Amer, "Optimum Grounding Grid Design by Using an Evolutionary Algorithm," IEEE General Meeting, Tampa, Florida, USA, 2007.